# The Characterization of Eutectic Al-Si Casting Alloy with Addition of Tin

**Kayvan Khatibi**

Submitted to the
Institute of Graduate Studies and Research
in partial fulfillment of the requirements for the degree of

Master of Science
in
Mechanical Engineering

Eastern Mediterranean University
September 2019
Gazimağusa, North Cyprus

Approval of the Institute of Graduate Studies and Research

Prof. Dr. Ali Hakan Ulusoy
Acting Director

I certify that this thesis satisfies all the requirements as a thesis for the degree of Master of Science in Mechanical Engineering.

Assoc. Prof. Dr. Hasan Hacışevki
Chair, Department of Mechanical Engineering

We certify that we have read this thesis and that in our opinion it is fully adequate in scope and quality as a thesis for the degree of Master of Science in Mechanical Engineering.

Asst. Prof. Dr. Mohammed Bsher A. Asmael
Supervisor

Examining Committee

1. Assoc. Prof. Dr. Qasim Zeeshan

2. Asst. Prof. Dr. Mohammed Bsher A. Asmael

3. Asst. Prof. Dr. Ali Evcil

# ABSTRACT

Global warming and shortage of fossil fuel are the most important concerns about the need for improvement of fuel economy. While the aerospace and automotive industries still rely on steel, the drive to increase fuel efficiency and reduce $CO_2$ emissions has led to much wider use of aluminum.

Alloying aluminum with other elements like silicon helps to enhance its physical properties such as strength. Aluminum-silicon (Al-Si) alloys are the most important among casting alloys. The microstructure of Al-Si alloys is generally composed of the coarse plate-like eutectic silicon structure that makes these alloys have a fracture under tension or have a crack initiation. Therefore, the microstructure of these alloys must be modified by the addition of elements to get a fine silicon structure.

This study aims to investigate the influence of tin addition on the characteristic parameters of the solidification process, microstructure, and mechanical properties of the eutectic Al-Si casting alloy. To do so, tin with different concentrations is used, and samples are taken from the base alloy and alloys modified with different tin addition.

Within the study, the cooling curve of the solidification process of the samples was analyzed by using the Computer-Aided Cooling Curve Thermal Analysis (CA-CCTA). Later, the microstructure of the samples was analyzed by using Optical Microscopy (OM) and Scanning Electron Microscopy equipped with Energy Dispersive X-ray Spectroscopy (SEM/EDS). Finally, the mechanical properties (hardness) of the samples were analyzed by using the Vickers hardness test.

The results show that by increasing tin, the temperature of the Al-Si phase increased. When the temperature increased, the mean area of silicon particles also increased. It means that tin does not have any effect on the modification of this type of Al-Si alloy. Besides, by increasing tin, the temperature of the last solidification phase increased. The reaction temperature later was increased by the formation of intermetallic compounds. Because tin formed the intermetallic compound with aluminum and silicon. Also, hardness increasing with tin increasing was because of the solid and hard intermetallic compound formed between tin, aluminum, and silicon in the last solidification phase.

**Keywords:** Aluminum-Silicon Alloys, Tin, Thermal Analysis, Microstructure, Mechanical Properties.

# ÖZ

Küresel ısınma ve fosil yakıt kıtlığı, yakıt ekonomisinin iyileştirilmesine duyulan ihtiyaçla ilgili en önemli endişelerdir. Havacılık ve otomotiv endüstrileri hala çeliğe güvenirken, yakıt verimliliğini artırma ve $CO_2$ emisyonlarını azaltma dürtüsü, alüminyumun çok daha fazla kullanılmasına neden oldu.

Alüminyumun silikon gibi diğer elementlerle alaşımlanması, mukavemet gibi fiziksel özelliklerini geliştirmeye yardımcı olur. Alüminyum-silikon (Al-Si) alaşımları döküm alaşımları arasında en önemlileridir. Al-Si alaşımlarının mikroyapısı genellikle, bu alaşımların gerilme altında kırılmasına veya çatlak başlangıcına neden olan kaba plaka benzeri ötektik silikon yapısından oluşur. Bu nedenle, bu alaşımların mikroyapıları, ince bir silikon yapı elde etmek için elementlerin eklenmesiyle modifiye edilmelidir.

Bu çalışma, kalay ilavesinin ötektik Al-Si döküm alaşımının katılaşma sürecinin karakteristik parametreleri, mikroyapı ve mekanik özellikleri üzerindeki etkisini araştırmayı amaçlamaktadır. Bunu yapmak için, farklı konsantrasyonlarda kalay kullanılır ve baz kalaydan ve farklı kalay ilavesi ile modifiye edilmiş alaşımlardan örnekler alınır.

Çalışmada, numunelerin katılaşma işleminin soğutma eğrisi Bilgisayar Destekli Soğutma Eğrisi Termal Analizi kullanılarak analiz edildi. Daha sonra, numunelerin mikroyapısı Optik Mikroskopi ve Enerji Dispersif X-ışını Spektroskopisi ile donatılmış Taramalı Elektron Mikroskobu kullanılarak analiz edildi. Son olarak, numunelerin mekanik özellikleri (sertlik) Vickers sertlik testi kullanılarak analiz edildi.

Sonuçlar kalay arttıkça Al-Si fazının sıcaklığının arttığını göstermektedir. Sıcaklık arttığında, silikon parçacıklarının ortalama alanı da artmıştır. Bu, kalayın bu tip Al-Si alaşımının modifikasyonu üzerinde herhangi bir etkisinin olmadığı anlamına gelir. Ayrıca, kalay arttırılarak, son katılaşma fazının sıcaklığı arttı. Reaksiyon sıcaklığı daha sonra, intermetalik bileşiklerin oluşumu ile arttırıldı. Çünkü kalay alüminyum ve silikon ile metaller arası bileşiği oluşturdu. Ayrıca, kalay artışı ile artan sertlik, son katılaşma aşamasında kalay, alüminyum ve silikon arasında oluşan katı ve sert metaller arası bileşikten kaynaklanmaktadır.

**Anahtar Kelimeler:** Alüminyum-Silikon Alaşımları, Kalay, Isıl Analiz, Mikroyapı, Mekanik Özellikler.

*This thesis is dedicated to the memory of my beloved brother Dr. Kambiz. His legacy will live on in those who cherish his memory...*

# ACKNOWLEDGMENT

I would first like to thank my supervisor, Assist. Prof. Dr. Mohammed Bsher A. Asmael. The door to his office was always open whenever I ran into a trouble spot or had a question about my research or writing. He consistently allowed this thesis to be my own work, but steered me in the right direction whenever he thought I needed it. I genuinely appreciate his tireless work, and support.

How can I ever thank my dear friend, Dr. Amirhossein Roshani, who was always there when I needed help, guidance, and advice? On this strenuous journey, it was wonderful to be accompanied by a true friend, and a positive personality, one who seems to lack words of negation in his mental lexicon.

It would be inappropriate if I omit to mention the names of my dear friends, Dr. Ali Marefati, Dr. Majid Karimnejad, Dr. Danial Forghani, Dr. Masoud Teymourfamian, Dr. Ehsan Bahramzadeh, Dr. Maryam Payghami, Dr. Mobina Beheshti, Dr. Vahid Khojasteh, Dr. John 'Femi Olaifa, Görkem Ozankaya, Saman Kanzi, and Pedram Lotfi who have, in their own ways, kept me going on my path to success, assisting me as per their abilities, in whatever manner possible and for ensuring that good times keep flowing.

I owe the greatest debt and gratitude to my dear girlfriend, who looked after me, encouraged me, and always stood by me. I could not have done it without you, Dr. Sara Kanzi.

Finally, nobody has been more important to me in the pursuit of this thesis than the members of my family. I must express my very profound gratitude to my beloved parents and to my brother, Kourosh for providing me with unfailing support and continuous encouragement throughout my years of study and through the process of researching and writing this thesis. This accomplishment would not have been possible without them. It really means a lot to me. Thank you.

# TABLE OF CONTENTS

# LIST OF TABLES

# LIST OF FIGURES

# LIST OF SYMBOLS AND ABBREVIATIONS

| | |
|---|---|
| $\Delta T$ | The Total Solidification Temperature |
| $\Delta t$ | The Total Solidification Time |
| $\Delta T_R$ | Recalescence Temperature |
| $\Delta t_R$ | Recalescence Time |
| $\Delta T_U$ | Undercooling Temperature |
| $\Delta t_U$ | Undercooling Time |
| AA | Aluminum Association |
| CA-CCTA | Computer-Aided Cooling Curve Thermal Analysis |
| CR | Cooling Rate |
| DCP | Dendrite Coherency Point |
| DSC | Differential Scanning Calorimetry |
| DTA | Differential Thermal Analysis |
| EDS | Energy Dispersive X-ray Spectroscopy |
| HV | Hardness Value |
| OM | Optical Microscopy |
| SD | Standard Deviation |
| SEM | Scanning Electron Microscopy |
| TGA | Thermo Gravimetry Analysis |
| $T_G$ | Growth Temperature (or Maximum Temperature) |
| $t_G$ | Growth Time |
| $T_{min}$ | Minimum Temperature |
| $t_{min}$ | Minimum Time |
| $T_N$ | Nucleation Temperature |

| | |
|---|---|
| $t_N$ | Nucleation Time |
| $T_S$ | Solidus Temperature |
| $t_S$ | Solidus Time |
| wt. | Weight Percent (or Percentage by Weight) |

# Chapter 1

# INTRODUCTION

## 1.1 Background

Global warming and lack of fossil fuel are the most important concerns about increasing the need for improvement of fuel economy. Indeed, reducing the weight of vehicles and developing the powertrain systems like hybrid motors are the primary key in this regard. So aluminum castings play a significant role in the automotive industry. Also, the use of aluminum castings is quite widespread in the aerospace industry. Because by making complex components lighter, not only production cost decreases, but also fuel economy increases. Therefore, aluminum and aluminum castings are used in a great variety of applications due to their unique advantages such as being lightweight, good electrical and thermal conductivity, good reflectivity, etc. Although the advantages of aluminum are greater than other metals, some developments in manufacturing and materials science of metals like steel challenge some of these advantages of aluminum [3,4,5].

Besides, the worldwide need for aluminum is increasing annually. Along with using virgin aluminum, aluminum industries are using recycled aluminum as well for not only decreasing the harmful impacts of these materials on the environment but also saving energy and cost. In addition, there is not any difference between secondary and new aluminum in quality [4,8].

In the aluminum industry, different elements are used as additives in Al-Si alloys that can be divided into major elements, minor elements, and impurity elements [12,13]. Major elements like Si are added to enhance the physical and mechanical characteristics of the alloy and also improve the phase modification, microstructure refinement, and heat treatment [10-14]. Minor elements like Ti are added to enhance the integrity (like wear, porosity, etc.) and also mechanical characteristics of the alloy [10-14]. Impurity elements like Fe are generally undesirable. These elements are usually used for recycled alloys. The presence of them has some advantages. Perhaps this keeps good mechanical properties and reduces their price [11].

Along with the addition of alloying elements, modification treatment also alters the eutectic Si morphology from acicular/flake to globular/fibrous [20]. As well as that, it makes some improvements to the mechanical attributes of aluminum-silicon alloys such as strength, elongation, and ductility [21]. Modification treatment is categorized into 3 different methods: (1) The chemical method in which modification of eutectic Si is done by adding some elements as modifiers to a molten Al-Si alloy like Na, and Sr. (2) The mechanical method which is based on breaking up plate-like silicon phases and α-Al dendrites by force. (3) The last two methods usually are combined and make the third method, thermal modification for the optimal mechanical properties of the alloy. This method consists of rapid cooling (solidification) of alloy for modifying [22].

Additionally, thermal analysis is a powerful method to determine the characteristics of Al-Si casting alloys such as latent heats, transformation temperatures, etc. This method is used usually during cooling or heating (solidification or melting, respectively). The most common techniques are DSC, DTA, TGA, and CA-CCTA [5]. Techniques like

DSC, DTA, and TGA are accurate, but they need laboratory equipment and samples with small size are used for them. To increase the measurement accuracy, the size of samples must be big enough and solidify over enough time. Therefore, the non-equilibrium technique is used like CA-CCTA [35]. This technique depends on interpreting and recording the temperature changes over time during solidification, which is known as the cooling curve. Using the cooling curve is not only easy and inexpensive but also suitable for industrial applications [36]. Alongside the cooling curve, understanding its derivative curves are also important. The derivative curves are the functions of slope changes, and these changes are the results of phase transformations [32-34].

## 1.2 The Problem Statement

Among casting alloys, Al-Si alloys are very popular because of their vast applications. Their unique casting characteristic parameters compared to other casting alloys, making them the most important industrial casting alloys [10,11].

Microstructure and mechanical properties are two essential requirements to produce Al-Si alloys with high quality. Several parameters, such as characteristics of solidification, heat treatment, the chemical composition of the alloy, and elements addition in the form of additives or modifiers strongly affect the mechanical properties and microstructure of Al-Si alloys. Development of the microstructure during the solidification depends on two factors: (1) The thermal conditions, (2) The melt modification and nucleation potentials [5]. The microstructure of aluminum-silicon eutectic alloys with approximately 12.3 wt.% silicon is generally composed of the coarse plate-like lamellar or acicular eutectic Si structure that makes these alloys have a fracture under tension or have a crack initiation. Therefore, to prevent these problems, the microstructure of these alloys must be modified by the addition of elements or processing alternatives to get a fine silicon structure such as the fine fibrous or globular [4].

## 1.3 Objectives of the Study

1) To investigate the influence of tin (Sn) addition with different concentrations on the characteristic parameters of the solidification of eutectic Al-Si casting alloy.
2) To investigate the influence of tin (Sn) addition with different concentrations on the microstructure of eutectic Al-Si casting alloy, then correlating the results with the results of the thermal analysis.
3) To investigate the influence of tin (Sn) addition with different concentrations on the mechanical properties of eutectic Al-Si casting alloy, then correlating the results with the results of the thermal analysis and microstructural analysis.

## 1.4 Scope of the Study

1) As a base alloy, eutectic Al-Si casting alloy (ETIAL-140) and in the form of additive, tin (Sn) with different concentrations (0.1%, 0.5%, and 1%) will be used.
2) Cooling curve of the solidification process of the base alloy and alloys modified with different Sn addition according to recorded data (temperature versus time) will be plotted and analyzed by using Computer-Aided Cooling Curve Thermal Analysis (CA-CCTA) technique.
3) The microstructure of the base alloy and alloys modified with different Sn addition will be analyzed by using Optical Microscopy (OM) (for measuring the size and shape of the eutectic Si structure) and Scanning Electron Microscopy equipped with Energy Dispersive X-ray Spectroscopy (SEM/EDS) (for mapping the chemical composition of the alloy along with its spectrum).

4) The mechanical properties (hardness) of the base alloy and alloys modified with different Sn addition will be analyzed by using the Vickers hardness test (for measuring the hardness values).

## 1.5 Organization of the Study

This study is organized in 5 chapters. Introduction, Literature review, Methodology, Results and Discussion, and Conclusion, respectively. The introduction chapter consists of a background of the study, problem statement, objectives, and scope of the study. The literature review chapter provides a concise but detailed and informative review on Al and Al alloys along with their advantages, their designation systems, and their applications. In addition, it reviews Al-Si alloys alongside their properties, their modification and common chemical modifiers, and their applications. Plus, this chapter examines the effect of elements on mechanical properties and microstructure of Al-Si alloys. Furthermore, it discusses the solidification of Al-Si alloys and phase formation during the solidification. Finally, this chapter considers thermal analysis as well as Computer-Aided Cooling Curve Thermal Analysis (CA-CCTA) technique, and how to use it for recognizing the phase transformation, and characteristic parameters. The methodology chapter presents the experimental procedure of this study. Also, in this chapter, the research method is explained and setting up all experiments and testing them, including materials preparation, thermal analysis, microstructure, and mechanical properties is covered. The results and discussion chapter discusses the recorded data from all experiments carried out in chapter three. In this chapter, the results of the base alloy and alloys modified with different Sn addition for thermal analysis, as well as microstructure and mechanical properties, are evaluated. Moreover, all the data-correlation is assessed. The conclusion chapter lists the conclusions of the study.

# Chapter 2

# LITERATURE REVIEW

## 2.1 Introduction

This chapter represents a literature review of aluminum alloys, aluminum-silicon casting alloys, and their properties according to metallurgical parameters. Then, the addition of some elements regarding their effects on the mechanical properties, microstructure, and solidification of these alloys will be covered. Finally, the significance of thermal analysis and its practical applications in engineering, especially materials science, will be discussed.

## 2.2 Aluminum and Aluminum Alloys

After oxygen and silicon (with 46.6% and 27.7% by mass respectively), aluminum is the third abundant element in the crust of Earth (with 8.1% by mass). However, in nature, aluminum exists just in the form of stable combinations with other materials, especially as oxides and silicates. Aluminum was established for the first time in 1808. L.B.G de Moreveau proposed the name alumina in 1761 according to the base in alum (a Latin word) but was used later in 1787 for the oxide of aluminum. Eventually, aluminum was proposed by Sir Humphery Davy in 1807 to agree with most of the elements which end with "ium" [1,2].

There are a lot of reasons that aluminum has been expanded into broader and newer fields of applications such as high level of thermal conductivities, lightweight, excellent corrosion resistance, high level of reflectivity, excellent workability, attractive appearance and other important properties which makes aluminum more practical than other elements. However, some disadvantages of aluminum like poor castability and low strength restrict its performance. For example, in the production of rotor castings of electrical motors. Usually, by adding alloying elements to aluminum can enhance the properties of it. Some major elements like Si, Cu, Mg, Zn, Li, Mn, and Ni can be added and then subjecting the aluminum to various mechanical, thermo-mechanical, and thermal treatments. Some minor elements like Sr, Na, Sb, Ba, and Ca can be added to make some changes in microstructure [4,7].

### 2.2.1 Advantages of Aluminum

**I) Density:** Aluminum with a density of 2.7 gr/cm$^3$, around one-third of copper (8.96 gr/cm$^3$) or steel (8.05 gr/cm$^3$), is one of the lightest metals. The result of high strength to weight ratio makes aluminum one essential structural material in transportation for increasing payloads or saving fuel [4,8].

**II) Strength:** Although pure aluminum does not have high strength, the addition of some alloying elements, as mentioned before, can increase the strength. Also, in cold weather, aluminum has an advantage over steel. In this condition, strength increases when temperature decreases while retaining its toughness. But steel at low temperature becomes brittle [4,8].

**III) Corrosion Resistance:** When aluminum exposed to air, almost instantaneously an oxide coating forms on the surface of it. This layer is highly protective and excellent for corrosion resistant. Although it is less resistant to alkalis, it relatively resists to most acids [4,8].

**IV) Thermal Conductivity:** The thermal conductivity of aluminum is almost twice and three times greater than copper and steel, respectively. It makes aluminum a good conductor for both heating and cooling applications. Because of its non-toxicity and thermal conductivity, Aluminum is used in utensils and kitchenware [4,8].

**V) Electrical Conductivity:** Although copper has a conductivity of 161% compared to aluminum and is widely used as a conductor, the electrical conductivity of aluminum is high as well, makes it a good electrical conductor [4,8].

**VI) Reflectivity:** Aluminum is a great reflector of radiant energy, from UV to infrared. The Combination of this property with being lightweight makes aluminum ideal for things like rescue blanket or light fixture. Also, because of the same property, aluminum is perfect for insulating material, in winter to insulate against heat loss and in summer to protect against the sun's rays [4,8].

**VII) Recyclability:** The worldwide need for aluminum is approximately 29 million tonnes annually. About 7 million tonnes are recycled from aluminum scrap, and 22 million tonnes are new aluminum. It only takes 700 kWh to recycle one tonne of aluminum. While producing one tonne of new aluminum takes 14000 kWh, and also, there is not any difference between recycled and virgin aluminum in quality. It means that using recycled aluminum is environmentally and economically compelling [4,8].

And other advantages of aluminum like impermeable, odorless, ductility and formability [9], workability, energy absorption capacity, fracture and cryogenic toughness, and ease of joining [3].

### 2.2.2 Aluminum Alloys Designation Systems

Aluminum alloys are widely used, and because of their broad applications in the worldwide, one system has been established by the Aluminum Association (AA) to manage and classify them. This organization uses two designation systems for two groups of aluminum alloys: wrought and cast aluminum alloys. The designation system which is used for wrought aluminum alloys is similar to cast aluminum alloys but with a few important differences. These designation systems consist of 4 numerical digits, sometimes with alphabetic suffixes or prefixes (Table 2.1). The designation system which is used for cast aluminum alloys has a decimal point after the third digit. In this system, the fourth digit is used to identify different forms of alloys: castings (0) or foundry ingots (1 or 2) [3,5].

Table 2.1: Designation System for Aluminum Alloys according to AA [3, 5]

| **Wrought aluminum alloys** | | **Cast aluminum alloys** | |
|---|---|---|---|
| **Main alloying elements** | **Alloy series** | **Main alloying elements** | **Alloy series** |
| More than 99% Al, Pure Al | 1xxx | More than 99% Al, Pure Al | 1xx.x |
| Cu | 2xxx | Cu | 2xx.x |
| Mn | 3xxx | Si + Cu and/or Mg | 3xx.x |
| Si | 4xxx | Si | 4xx.x |
| Mg | 5xxx | Mg | 5xx.x |
| Si + Mg | 6xxx | Unused series | 6xx.x |
| Zn | 7xxx | Zn | 7xx.x |
| Other elements | 8xxx | Sn | 8xx.x |
| Unused series | 9xxx | Other elements | 9xx.x |

### 2.2.3 Applications of Aluminum Alloys

The important applications of aluminum alloys are categorized according to their type and class, as discussed in the previous section in two tables below (Table 2.2 and Table 2.3). This review gives a clear understanding of the major characteristics of the various aluminum alloys such as strength, heat treatable, fluidity, machinability, etc. and demonstrates the applications for specific needs [18].

Table 2.2: Applications for Wrought Aluminum Alloys [18]

| Alloy | Major characteristics | Applications |
|---|---|---|
| 1xxx | 1) Strain hardenable<br>2) High formability, corrosion resistance, and electrical conductivity<br>3) Readily joined by welding, brazing, and soldering | Food packaging trays of pure aluminum, decorated foil pouches for food and drink, aluminum foil of CP aluminum, and pet food decorated wrap |
| 2xxx | 1) Heat treatable<br>2) High strength, at room and elevated temperatures<br>3) Usually joined mechanically, but some alloys are weldable | Aircraft internal and external structures, structural beams of the heavy dump and tank trucks and trailer trucks, the fuel tanks and booster rockets of the space shuttle, and internal railroad car structural members |
| 3xxx | 1) High formability and corrosion resistance with medium strength<br>2) Readily joined by all commercial procedures | Automotive radiator heat exchangers, tubing in commercial power plant heat exchangers, and the bodies of beverage cans |
| 4xxx | 1) Heat treatable<br>2) Good flow characteristics, medium strength<br>3) Easily joined, especially by brazing and soldering | Forged aircraft pistons, and structural and automotive applications |
| 5xxx | 1) Strain hardenable<br>2) Excellent corrosion resistance, toughness, weldability; moderate strength<br>3) Building and construction, automotive, cryogenic, and marine applications | Highway structures, including bridges, storage tanks, and pressure vessels, cryogenic tankage, systems for temperatures as low as −270 °C or near absolute zero, and marine applications |
| 6xxx | 1) Heat treatable<br>2) High corrosion resistance, excellent extrudability; moderate strength<br>3) Readily welded by GMAW and GTAW methods | In welded structural members such as truck and marine frames, railroad cars, pipelines, in the structural members of wide-span roof structures for arenas and gymnasiums, and geodesic domes |
| 7xxx | 1) Heat treatable<br>2) Very high strength; special high toughness versions<br>3) Mechanically joined | Critical aircraft wing structures of integrally stiffened aluminum extrusions, and long-length drill pipe |
| 8xxx | 1) Heat treatable<br>2) High conductivity, strength, and hardness | Electrical conductors, and aerospace applications |
| 9xxx | - | - |

Table 2.3: Applications for Cast Aluminum Alloys [18]

| Alloy | Major characteristics | Applications |
|---|---|---|
| 1xx.x | - | - |
| 2xx.x | 1) Heat treatable sand and permanent mold castings 2) High strength at room and elevated temperatures; some high toughness alloys | For engine piston heads, integral engine blocks, or bearings, and aircraft components |
| 3xx.x | 1) Heat treatable sand, permanent mold, and die castings 2) Excellent fluidity, high strength, and some high toughness alloys 3) Readily welded | Inner turbo frame for the Airbus family of aircraft, the gearbox casing for a passenger car, and rear axle housing |
| 4xx.x | 1) Non-heat-treatable sand, permanent mold, and die castings 2) Excellent fluidity, good for intricate castings | Complex cast parts for typewriter and computer housings and dental equipment, and also for fairly critical components in marine and architectural applications |
| 5xx.x | 1) Non-heat-treatable sand, permanent mold, and die castings 2) Tougher to cast; provides good finishing characteristics 3) Excellent corrosion resistance, machinability, and surface appearance | Suitable for components exposed to seawater or to other similar corrosive environments. used for door and window fittings, which can be decoratively anodized to give a metallic finish or provide a wide range of colors |
| 6xx.x | - | - |
| 7xx.x | 1) Heat treatable sand and permanent mold castings (harder to cast) 2) Excellent machinability and appearance | Furniture, garden tools, office machines, farming, and mining equipment |
| 8xx.x | 1) Heat treatable sand and permanent mold castings (harder to cast) 2) Excellent machinability 3) Bearings and bushings of all types | For parts requiring extensive machining and for bushings and bearings |
| 9xx.x | - | - |

## 2.3 Aluminum-Silicon Alloys

Among casting alloys, aluminum-silicon alloys are the most important ones and have a lot of applications such as in the automotive industries and aerospace industries [10,11]. The Al-Si foundry alloys are the dominant alloys that contain silicon between

5 and 25 wt.%. Other additives are Cu, Ni, and Mg. The Al-Si alloys microstructure is made of a primary phase (α-Al for hypoeutectic or primary Si for hypereutectic), Al-Si eutectic, Ni, Mg, Fe, and Cu-rich phases [11,12]. Al-Si alloys microstructure is shown in Figure 2.1.

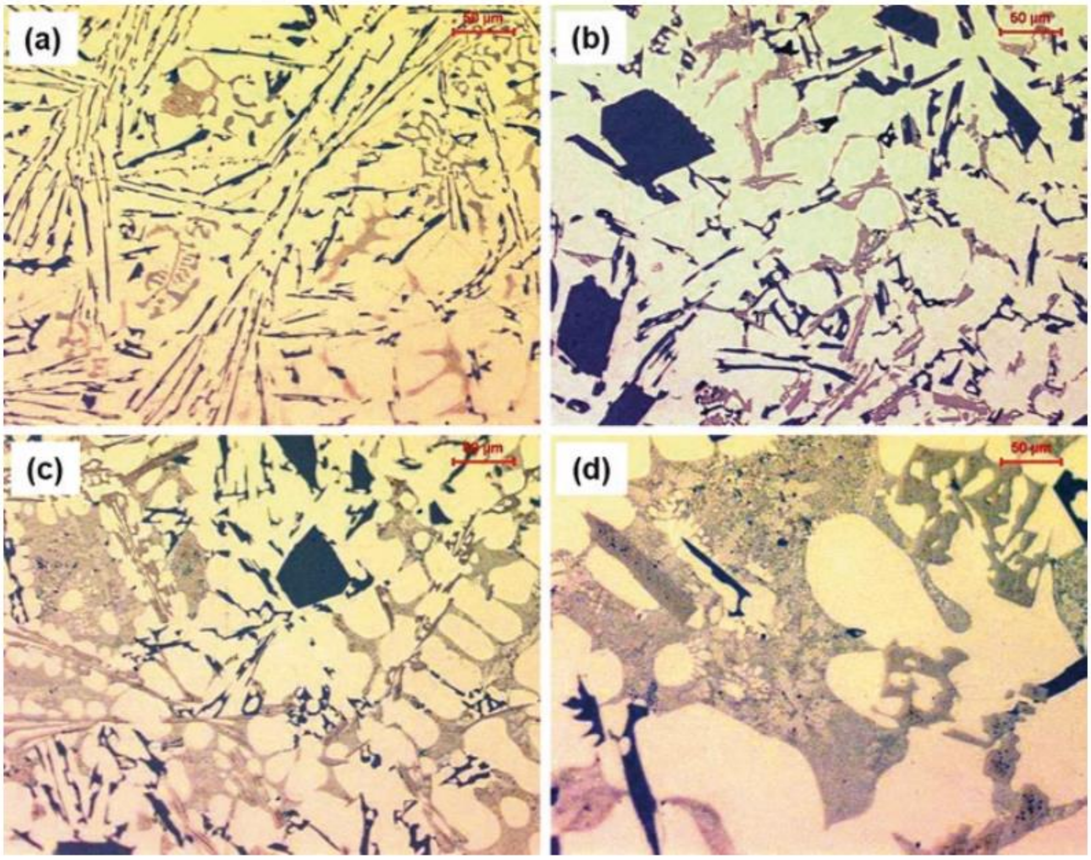


Figure 2.1: Al-Si Alloys Optical Microscopy for (a) Al-Si Hypoeutectic or Eutectic Alloys, (b) Al-Si Hypereutectic Alloys, (c) Dendritic Structure of Al-Si Hypereutectic or Hypoeutectic Alloys, and (d) Al-Cu Eutectic Alloys [5]

80-90% of all aluminum castings that are produced in the world is constituted by Al-Si castings [10,14,15]. Iron (Fe) forms detrimental intermetallics, which are brittle crystals, makes it the most undesirable or the main impurity element in Al-Si alloys [10,11]. By adding Manganese (Mn), detrimental Fe intermetallics transform into Chinese-script intermetallics that are less harmful [11,14]. A eutectic reaction that forms the binary system of Al-Si occurs at a temperature of 577 °C at 12.3 wt.% silicon

(Figure 2.2). Al-Si alloys are divided into three types according to their silicon percentage points: with more silicon than 12.3 wt.% are hypereutectic alloys, with less silicon than 12.3 wt.% are hypoeutectic alloys and with approximately 12.3 wt.% silicon are eutectic alloys [16].

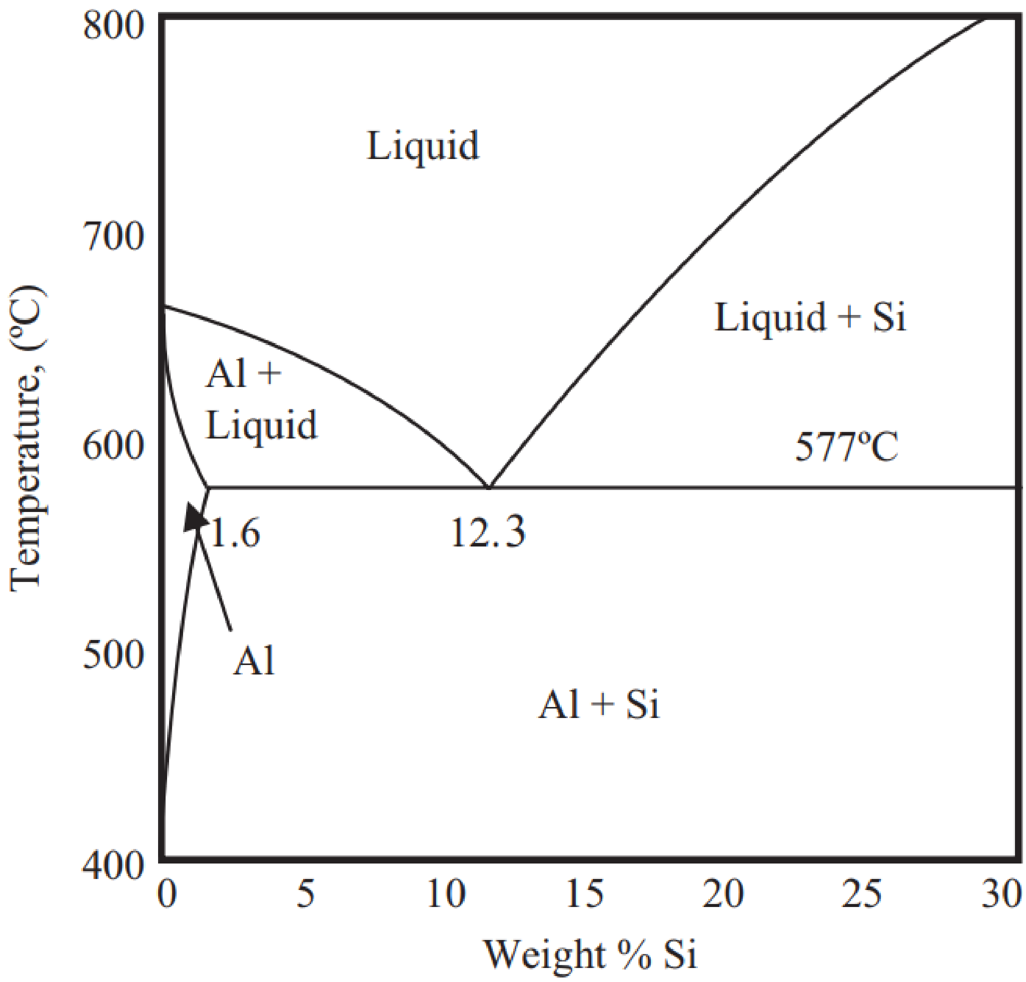

Figure 2.2: Phase Diagram of Al-Si Alloys [16]

### 2.3.1 Properties of Al-Si Alloys

Silicon has a significant role in all processes of aluminum castings. The addition of silicon in aluminum alloys has outstanding effects on their mechanical characteristics. The most important of them are covered below [4,5,19]:

1. Silicon improves hot tear resistance, fluidity, metal castability, and feeding characteristics dramatically.
2. Adding silicon to aluminum alloys makes them more resistant to cracking in solidification.
3. Adding silicon affects thermal and electric conductivity too and mostly depends on the amount of it that is used in the solution.
4. The silicon addition makes impact and creep resistance increase.
5. Silicon during solidification decreases metal shrinkage.
6. Silicon lowers thermal expansion as well as the lattice parameter slightly.
7. And finally, magnetic susceptibility and specific gravity are reduced by silicon.

### 2.3.2 Modification of Al-Si Alloys and Common Chemical Modifiers

Modification treatment alters the eutectic Si morphology from acicular/flake to globular/fibrous [20] and also it makes some improvements to the mechanical attributes of aluminum-silicon alloys such as strength, elongation, and ductility [21]. Modification treatment is categorized into three different methods: chemical, mechanical, and thermal methods. In the chemical method modification of eutectic Si is done by adding some elements as modifiers to a molten Al-Si alloy. This method is the best option for modification. The mechanical method is based on breaking up plate-like silicon phases and α-Al dendrites by force. The last two methods usually are combined and make the third method, thermal modification for the optimal mechanical properties of the alloy. This method consists of rapid cooling (solidification) of alloy for modifying [22]. The optical micrographs of Al-13Si with and without Na addition as a modifier are shown in Figure 2.3.

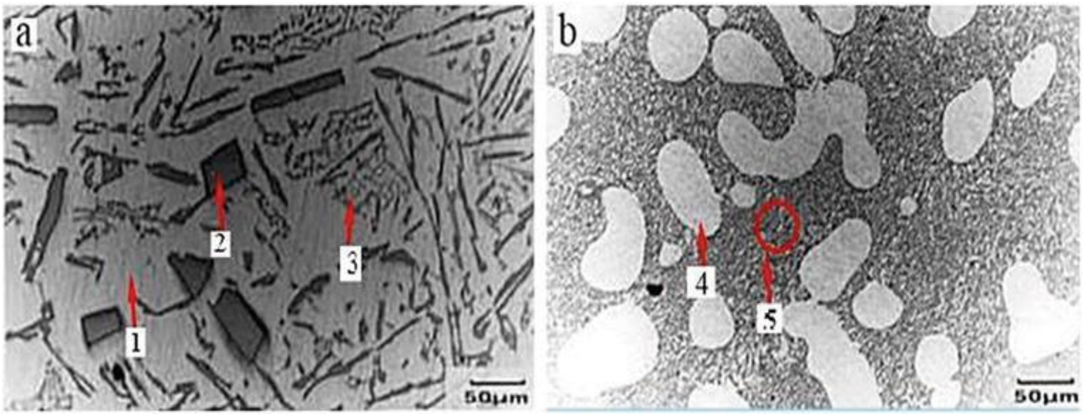

Figure 2.3: Optical Micrographs of (a) Al-13Si, and (b) Al-13Si-0.01Na; 1 = α-Al Dendrite; 2 = Primary Si; 3 = Eutectic Si; 4 = α-Al; and 5 = Fibrous Eutectic Si [23]

As mentioned before, some elements are used for modification. They are called chemical modifiers. The widely used and most common modifiers are antimony, strontium, and sodium [22]. They can be added to the molten alloys in 3 different ways: through fluxes, elements, and in the form of master alloys [20]. A finer fibrous or lamellar eutectic structure can be gotten by adding these chemical modifiers to Al-Si alloys. These additions either stop the silicon crystals' growth or balance the growth rates of silicon-matrix [4]. Modifiers, according to their type and their effects on the morphology of eutectic Si, are categorized in Table 2.4.

Table 2.4: Modifying Elements and their Effects [10,25,26]

| Elements | | Morphology of eutectic silicon |
|---|---|---|
| No addition | | - |
| The alkali metals | Na | Fibrous |
| | K | Fibrous |
| | Rb | Fibrous |
| Alkaline-earth metals | Ca | Fibrous |
| | Sr | Fibrous |
| | Ba | Fibrous |
| Rare-earth metals (Lanthanide) | Ce | Fibrous |
| | Eu | Fibrous |
| Group 15 of the Periodic Table (Pnictogen) | As | Lamellar (or a fine version of acicular) |
| | Sb | Lamellar (or a fine version of acicular) |
| Group 16 of the Periodic Table (Chalcogen) | Se | Lamellar (or a fine version of acicular) |
| Group 12 of the Periodic Table | Cd | Lamellar (or a fine version of acicular) |
| Rare-earth metals (Lanthanide) | La, Pr, Nd, Pm, Sm, Gd, Tb, Dy, Ho, Er, Tm, Yb, and Lu | Lamellar (or a fine version of acicular) |

### 2.3.3 Applications of Al-Si Alloys

The use of cast aluminum and application of its components is increasing over the years steadily to make aluminum the second abundant alloy (the first place belongs to iron and steel) [27]. As mentioned before, aluminum-silicon casting alloys have a lot of applications in the aerospace and automotive industries. Because cast aluminum has so many advantages, such as being lightweight, good electrical and thermal conductivity, good reflectivity, etc. [27,10]. Another important advantage of cast aluminum is recyclability, especially nowadays when recycling, environmental, and green energy awareness is of paramount importance [10,24,27].

Al-Si casting alloys with the silicon concentration less than 3% are used for marine fittings, with the silicon concentration between 3% and 5% are used for valve bodies, vessels, and fabricating rotors [20], with the silicon concentration between 11% and 13% are used in the aerospace and automotive industries, and with the silicon concentration more than 13% are used for tribological applications [39].

Most of the powertrain components in the automotive industry are manufactured with Al-Si casting alloys. For example, the automotive industry of North America has been converting cast productions from iron components to components made of cast aluminum alloys for many years. Right now, approximately 25% of the engine blocks and 80% of the engine heads are made from aluminum castings [24].

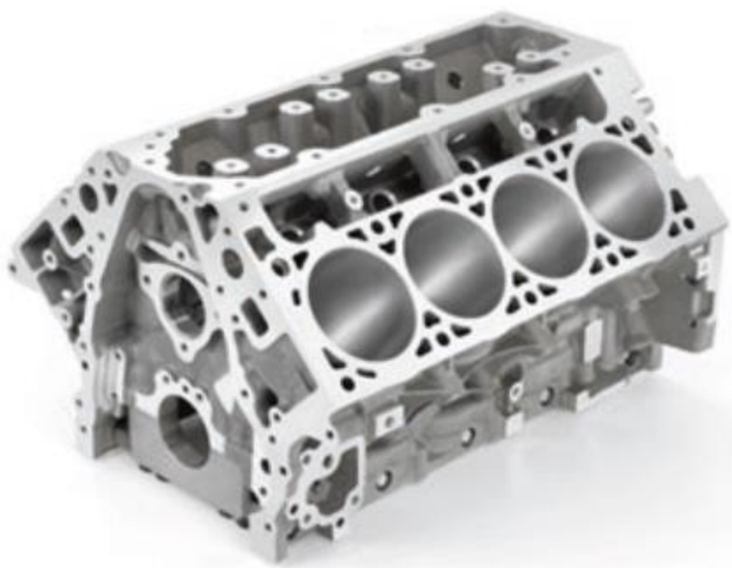

Figure 2.4: Engine Block of Corvette that is made by Sand Casting Process [5]

The significant increase in using Al-Si casting alloys in the aerospace industry is to make complex components lighter along with lower production cost and increased fuel economy. As an example, substructures made of aluminum wrought that are welded together and formed the desired shape. Today they are made from one single casting process. By removing welds, the weight is reduced by 50% [5].

Figure 2.5: Winglet Substructure of Embraer Phenom by using F357 Alloy that is made in the Investment Process [5]

## 2.4 Effect of Elements on Aluminum-Silicon Alloys

Al-Si alloys are divided mainly into new (primary) and recycled (secondary) alloys. Both of them have different elements that according to their capabilities, can be divided into major elements, minor elements, and impurity elements [12,13]. It should be considered that major elements in some alloys might be impurity elements in others [17]. Major elements (Si, Zn, Cu, Ni, and Mg) are added to enhance the physical and mechanical characteristics of the alloy. They have the potential to improve the phase modification, microstructure refinement, and heat treatment [10-14]. Minor elements (rare elements, P, B, Ti, and Sr) are added to enhance the integrity (like wear, porosity, etc.) and also mechanical characteristics of the alloy [10-14]. Impurity elements (Mn, Sn, Sb, Pb, and Fe) as mentioned before, are generally undesirable. These elements are usually used for recycled alloys. The presence of them has some advantages. Perhaps this keeps good mechanical properties and reduces their price [11]. In the next sections, the influence of these elements, especially tin (Sn) on the mechanical properties and microstructure, will be discussed in detail.

### 2.4.1 Effect on Mechanical Properties

Mohamed et al. [44] reported the effects of tin on the Al-Si-Cu-Mg and Al-Si-Mg alloys. They noticed adding 0.15% Sn decreased tensile (UTS and YS) and hardness and increased toughness and ductility of both B319.2 and A356.2 alloys (as-cast). Mechanical properties of both B319.2 and A356.2 alloys (heat-treated) by increasing Sn content decreased, may be attributed to the β-Sn and $Mg_2Sn$ phases formation.

Ahmad et al. [45,46] systematically investigated the effect of adding lanthanum and cerium on the eutectic Al-Si-Cu-Mg alloy. They discovered by adding 0.1% La, the base alloy quality index and ultimate tensile strength (UTS) increased. Also by increasing La content, elongation to fracture (except for 0.8% La addition) and hardness increased. About Ce, by adding 0.1% Ce, the base alloy quality index, and ultimate tensile strength (UTS) increased. However, there was not any improvement in the surface of ductile fracture by increasing Ce from 0.5% to 1.0%. Also, by increasing Ce content, hardness increased.

Zhiqiang Cao et al. [47] studied the effect of adding europium on A356 alloy (as-cast and heat-treated). They found out according to the quality index results, an optimal value (440 MPa) was the combination of elongation (14.7%) and UTS (265 MPa) in T6 heat treatment that was obtained by adding 0.1% Eu. The UTS and elongation increase of the A356 as-cast alloys accompanied the transfer after the modification from brittle to ductile mode. T6 heat treatment improved the UTS and elongation of A356 alloy significantly.

It has been reported by Jianhua Zhao et al. [48] the results of neodymium addition on Al-7Si-0.3Mg-0.3Fe alloy. They observed that according to the quality index results, an optimal value (375 MPa) was the combination of elongation (3.1%) and UTS (302 MPa) in T6 heat treatment that was achieved by adding 0.03% Nd. As Nd increased, mechanical properties due to the coarse particles of Nd-rich decreased in both as-cast and heat-treated.

It has been investigated by Cong Xu et al. [49] the results of scandium addition on F357 alloy. They noticed the right combination between YS, UTS, and elongation in T6 heat treatment was obtained by adding 0.8% Sc.

It has been studied by B.S. Murty et al. [50] the results of adding scandium on A356 alloy. They discovered the 0.4% Sc addition improved the UTS (25%), hardness (20%), and ductility (30%) in as-cast. This improvement may be ascribed to the effect of phase modification, eutectic Si modification, and grain refinement together.

### 2.4.2 Effect on Microstructure

Mohamed et al. [44] reported that in the B319.2 alloy, Sn precipitates like $Mg_2Sn$ particles (on the eutectic Si particles) and Sn particles (β-Sn in the $Al_2Cu$ network). In the A356.2 alloy, Sn precipitates like $Mg_2Sn$ particles (in the form of Chinese script). Concerning the addition of Sn, the $Mg_2Si$ phase has a considerable amount of Sn that alters the phase composition to $Mg_2Si_{0.2}Sn_{0.8}$.

Farahany et al. [51,52] investigated that the bismuth and antimony presence in the molten Al-Si (ADC12 die casting alloy) neutralized the strontium effect as a modifier by increasing the $T_N$ and $T_G$ for eutectic Si phase. Also, for Sr/Bi and Sr/Sb ratio around 0.5 below which the strontium modification efficiency is lost, and the flake-like unmodified structure of silicon is formed.

Ahmad et al. [53] noticed that after increasing cerium content to the Al-11.7Si-2Cu-Mg alloy, the $T_N$, $T_{min}$, and $T_G$ decreased. Also, the area of silicon particles reduced at Ce high levels (1.0%). The silicon structure refinement can be seen at Ce addition up to 1.0%. Ce formed intermetallic compounds like Al-Si-Cu, which had plate-like structures. They affected the base alloy modification. With the increasing of Ce content, the $T_N$ and $T_G$ of the last Al-Cu solidification phase increased, which Ce altered the Al-Cu phase morphology to needle-shaped Al-Si-Cu-Ce.

Also, Ahmad et al. [45] discovered that after increasing lanthanum up to 1.0% to the Al-11.7Si-2Cu-Mg alloy, the $T_N^{Al\text{-}Si}$ and $T_G^{Al\text{-}Si}$ decreased although the $\Delta T_R$ increased. Also, the area of silicon particles reduced at La high levels (1.0%). With the increasing of La content, the $T_N$ and $T_G$ of the last Al-Cu solidification phase increased.

Tongmin Wang et al. [54] found out that after increasing phosphorus content to the Al-7Si alloy, the $T_N$, $T_{min}$, and $T_G$ increased although $\Delta T_R$ decreased regardless of europium concentration. However, $\Delta T_R$ increased by increasing Eu content. Both $T_N$ and $T_{min}$ decreased by increasing Eu content, in the case of high P concentrations (5 and 30 ppm).

Zhi Hu et al. [55] observed that after increasing ytterbium content to the Al-10Si alloy, the $T_N$, $T_{min}$, and $T_G$ decreased. Also, according to the cooling curve, $\Delta T_R$ reached the maximum temperature (2.3 °C) with 0.7% Yb addition. In the Yb-modified alloys, the eutectic Si morphology changed to a fine fibrous honeycomb structure from a coarse plate-like structure, and the intermetallic compound of Al-Si-Yb is formed in the Yb-modified alloys.

Zhiqiang Cao et al. [47] reported that after adding europium content to the A356 alloy, the eutectic Si particles size reduced and by increasing it, the refinement effect improved. The 0.1% Eu addition changed the morphology of eutectic Si to a fine fibrous and fully modified form from a coarse plate-like one. With increasing Eu content, the $T_N$, $T_{min}$, and $T_G$ decreased although $(\Delta T_U)_N$ and $(\Delta T_U)_G$ increased. $\Delta T_R$ increased by initial Eu addition, but it remained stable for further additions (above 0.06% Eu).

Jianhua Zhao et al. [48] investigated that after adding 0.03% neodymium to the Al-7Si-0.3Mg-0.3Fe alloy, the β-AlFeSi phase and the Nd-rich particles were detected in the alloy. By increasing Nd content, the Nd-rich particles attached to the β-AlFeSi phase surface. After T6 heat treatment, the size of these particles decreased, and their morphology changed to spherical and fragmented form. Also, the Nd addition affected the π-AlSiMgFe phase as well. With 0.03% Nd addition, alloy showed the maximum $\Delta T_U$ and had an optimal state for this phase formation. By increasing the Nd content, the Nd-rich particles decreased the π-AlSiMgFe phase amount on the β-AlFeSi phase.

Cong Xu et al. [49] noticed that scandium has a lot of refining effects on the as-cast F357 alloy microstructure such as β-$Al_5FeSi$ phase disposal and eutectic Si modification. T6 heat treatment on alloys with Sc modification in comparison with alloys without modification induces the eutectic Si fragmentation and spheroidization, as well as $Al_3Sc$ dispersoids precipitation.

B.S. Murty et al. [50] discovered that after adding a 0.4% scandium to the A356 alloy, the morphology of silicon changed from a plate-like form to a globular and fibrous one. After T6 heat treatment, the morphology of eutectic Si changed to a fibrous form in the A356 alloy, and a globular form in Sc modified alloy. Also, with Sc addition, the irregular $\pi$-$Al_8Mg_3Si_6Fe_1$ and the needle-like $\beta$-$Al_5FeSi$ phases modified to irregular shaped fine-sized $\pi$-$Al_8Mg_3(Si, Sc)_6Fe_1$ and $\beta$-$Al_5Fe(Si, Sc)$ particles. Besides, the V-$AlSi_2Sc_2$ phase was spotted in the Sc modified alloy.

F. H. Samuel et al. [56] found out that after adding beryllium content to the B356 and B357 alloys, the script-like Be-Fe phase precipitated at β-platelets or close to it. One new reaction that took place near the end of the solidification process was spotted, which is made of silicon particles and $\pi$-$Al_8Mg_3FeSi_6$ phases.

## 2.5 Solidification of Aluminum-Silicon Alloys and its Phase Formation

Before the discussion about solidification, it would be essential to understand the phase formation of Al-Si casting alloys and the order of the formation first. The solidification of alloys is monitored via the thermal analysis method by using a thermocouple [28,29]. The thermal analysis curve of one type of casting alloy and its dT/dt curve with the phase evolution and arrest points identification is shown in Figure 2.6.

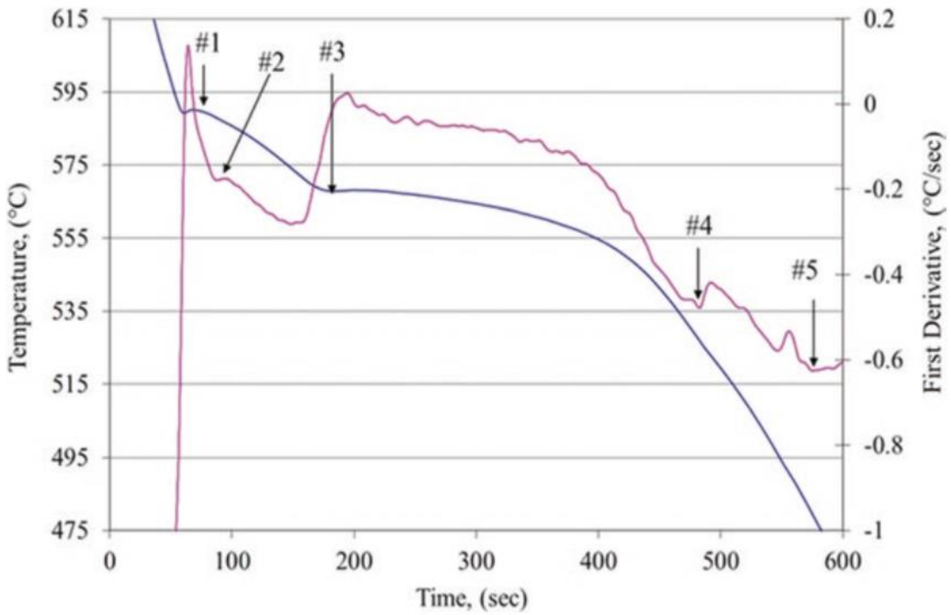

Figure 2.6: Cooling Curve of the 319-type Casting Alloy along with its First Derivative Curve. The Solidification Rate of the Test Sample was 0.15 °C/s [5]

Arrest points are temperature points at which certain property changes occur and are identified in the calculated dT/dt curve, which is specified from the cooling curve [28-31]. The arrest points according to their sequence are listed below:

1. The first arrest point (#1) is related to the α-Al phase nucleation (liquidus).
2. The second one (#2) is associated with the growing α-Al phase, which contacts with near α-Al crystals (also known as DCP = The Dendrite Coherency Point).
3. The third one (#3) is related to the formation of the main Al-Si eutectic structure during the progress of solute enrichment.
4. The fourth one (#4) is related to the formation of the Al-Cu-Mg-Fe-Si and Al-Cu-Si reactions after enriching the remaining liquid in Si, Mn, Fe, Mg, and Cu.
5. The last point (#5) is associated with the end of solidification (solidus).

During the phase formation of Al-Si alloys energy generates as latent heat, which makes inflection points. They change the cooling curve slope (Figure 2.7). Also, it exhibits three major metallurgical reactions. So, the phase formation of Al-Si alloys during the solidification process consists of these three reactions [42]:

1. Primary Al dendrite network formation for the first solidification stage
2. Al-Si eutectic phase formation
3. Eutectic intermetallic compound formation for the last solidification stage

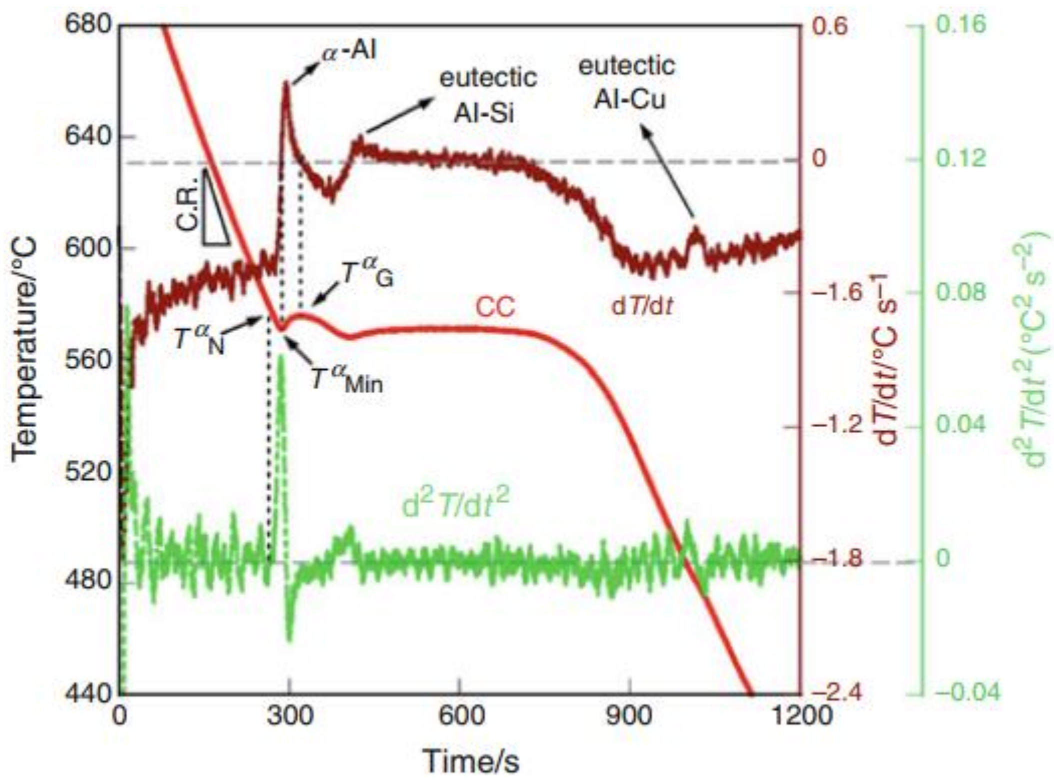


Figure 2.7: Cooling Curve of Al–11.3Si–2Cu–0.4Fe Alloy along with its corresponding Derivative Curves [42]

## 2.6 Thermal Analysis

Thermal analysis is a powerful method to determine the characteristics of Al-Si casting alloys such as latent heats, fraction transforming, fraction solids, transformation temperatures, etc. This method is used usually during cooling or heating (solidification or melting, respectively). The most common technique is DSC (Differential Scanning Calorimetry), along with other techniques like DTA (Differential Thermal Analysis), TGA (Thermo Gravimetry Analysis), and CA-CCTA (Computer-Aided Cooling Curve Thermal Analysis) [5].

Thermal analysis gathers the precise data of the temperature changes. The study of these data is based on a clear understanding of the curves (heating or cooling) and the derivative curves (first and/or second). Derivative curves are the functions of slope changes, and these changes are the results of phase transformations. There is a direct link between the energy which is stored during the slope changes in them and the energy that is required for the transformation. It is called latent heat (for solidification, transformation, and melting) [32-34].

Thermal analysis is strongly supported by algorithms that help to determine the main properties of the cooling or heating curves. These algorithms are used to specify the baseline: Newtonian, Linear, Polynomial, and Fourier [5].

### 2.6.1 Computer-Aided Cooling Curve Thermal Analysis

Techniques like DSC, DTA, and TGA are accurate, but they need laboratory equipment, and samples with small size are used for them. To increase the measurement accuracy, the size of samples must be big enough and solidify over enough time. Therefore, the non-equilibrium technique should be used [35]. This technique depends on interpreting and recording the temperature changes over time during solidification, which is known as the cooling curve. Using the cooling curve is not only easy and inexpensive but also suitable for industrial applications [36]. Because of the ability of cooling curve that can be used during casting and melting, also this technique is called in-situ, in which the changes of temperature over time is recorded when one sample from fully liquid phase changes to fully solid phase and during that, a curve of temperature over time is plotted. For producing this type of curve, first, solid metal is melted and changed to liquid form. Then, is poured into a mold in which one or two thermocouples are inserted. The number of thermocouples that is used depends on the algorithm mentioned before [37]. In the thermal analysis, sensitive equipment is used to carry out a material thermal history like data acquisition systems. They are connected to the Computer and record the temperature of Al-Si alloys via thermocouples [5]. The analysis of the cooling curve and its derivative curves can be done by using suitable data analysis software, and the procedure of using it is known as CA-CCTA (Computer-Aided Cooling Curve Thermal Analysis) [37].

### 2.6.2 Recognition of Phase Transformation and Characteristic Parameters

The cooling curve and its derivative curves (first and second) provide useful information about phase identification. The first derivative represents the cooling rate in degrees per second, which offers some details about major reactions that cannot be spotted on the cooling curve [12]. The second derivative can be used to detect minor reactions like the formation of detrimental Fe intermetallics during phase transformation [38].

To describe the qualities of phase reactions, it is important to know several characteristic parameters: Growth (or maximum) temperature ($T_G$), Minimum temperature ($T_{min}$), Nucleation temperature ($T_N$), Solidus Temperature ($T_S$), Undercooling Temperature ($\Delta T_U$), Recalescence Temperature ($\Delta T_R$), and their corresponding times. These parameters are determined generally by the CA-CCTA technique (Table 2.5).

Table 2.5: Characteristic Parameters with their Symbols [38]

| Symbol | Description |
|---|---|
| $T_N$ | Nucleation Temperature |
| $t_N$ | Nucleation Time |
| $T_G$ | Growth Temperature (or Maximum Temperature) |
| $t_G$ | Growth Time |
| $T_{min}$ | Minimum Temperature |
| $t_{min}$ | Minimum Time |
| $T_S$ | Solidus Temperature |
| $t_S$ | Solidus Time |
| $\Delta T_U$ | Undercooling Temperature ($\Delta T_U = T_N - T_{min}$) |
| $\Delta t_U$ | Undercooling Time ($\Delta t_U = t_N - t_{min}$) |
| $\Delta T_R$ | Recalescence Temperature ($\Delta T_R = T_G - T_{min}$) |
| $\Delta t_R$ | Recalescence Time ($\Delta t_R = t_G - t_{min}$) |
| C.R. | Cooling Rate |

First of all, the mentioned parameters must be defined. Nucleation Temperature ($T_N$) is the temperature of the first silicon crystals when they nucleate and start to grow. Growth Temperature ($T_G$) which is the maximum temperature as well, is the temperature of the latent heat that releases during the phase transformation. In comparison with ($T_G$), ($T_{min}$) is the minimum temperature of reactions during the phase transformation. Solidus Temperature ($T_S$) is the temperature of the end of the solidification process. Undercooling ($\Delta T_U$) is a temperature drop under the equilibrium temperature approximately at the beginning of solidification. Recalescence ($\Delta T_R$) is a temperature rise due to the evolution of latent heat during the process [40].

Second, finding these parameters on the cooling curve and its first derivative curve is also important. The intersections of the zero line of the first derivative curve with the cooling curve are $T_G$ and $T_{min}$. These points can be determined as extremums on the first derivative curve, and as mentioned before, heat is released at these points [20]. For measuring $T_N$, the cross technique of two slope-tangents is employed on the first derivative curve, as shown in Figure 2.8 [40]. Undercooling is the subtraction of $T_N$ and $T_{min}$, and Recalescence is the subtraction of $T_G$ and $T_{min}$ [38].

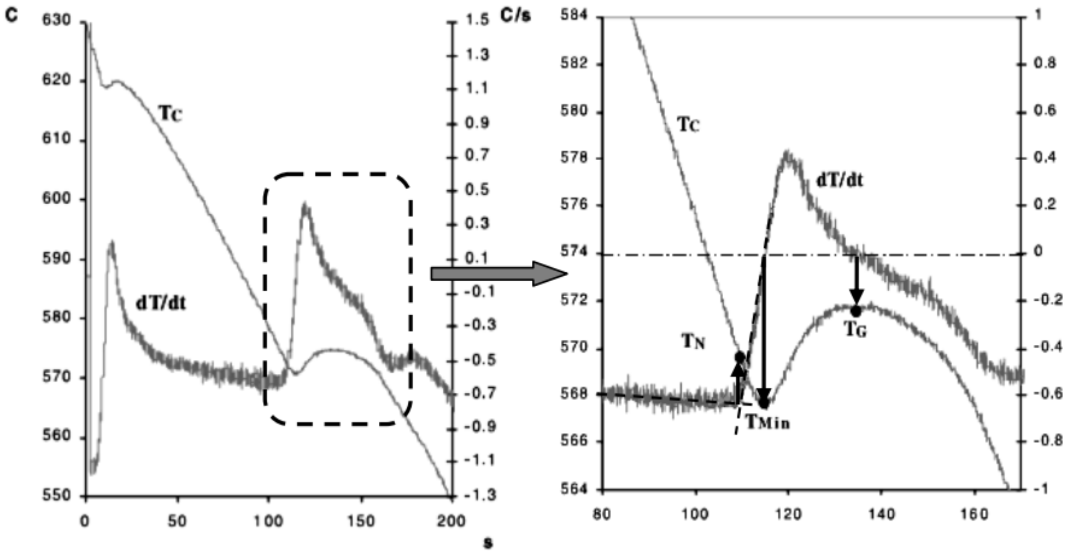


Figure 2.8: Position of the Characteristic Parameters ($T_N$, $T_G$, and $T_{min}$) and the Cross Technique of Two Slope-Tangents for measuring $T_N$ (A356 Alloy) [40]

The solidification of A356 alloy (Al-Si-Mg), does not finish at the Al-Si eutectic temperature and continues at lower temperatures. It is determined by the $Mg_2Si$ reaction, which is the secondary eutectic reaction. These reactions make the solidification process more complicated [41].

### 2.6.3 Approach for Analyzing the Second Derivative Curve

As mentioned before, the second derivative can be used to detect minor reactions like the formation of detrimental Fe intermetallics during phase transformation [38]. There is a moment for the cooling rate when it increases to a higher level. A minimum point of the second derivative was employed to spot this moment. A low correlation between grain size and characteristic parameters was obtained and imprecision to identify nucleation points in the solidification process could be caused by it [43].

# Chapter 3

# METHODOLOGY

## 3.1 Introduction

The experiments that were performed to achieve the objectives will be explained in detail, in this chapter. These experiments include preparation of materials used as a base alloy and an additive, melting and cooling processes, techniques used such as Computer-Aided Cooling Curve Thermal Analysis (CA-CCTA) for thermal analysis, Optical Microscopy (OM) and Scanning Electron Microscopy equipped with Energy Dispersive X-ray Spectroscopy (SEM/EDS) for microstructure analysis, and finally mechanical properties testing. The base alloy used in this research supplied by Tuncel Metal Ltd. The chemical composition of the alloy is shown in Table 3.1. According to the Si content, this alloy categorized as a eutectic alloy.

Table 3.1: Chemical Composition of the Al-Si Alloy used in this Research

| **Commercial Name:** ETIAL-140 | | | | | | | | | |
|---|---|---|---|---|---|---|---|---|---|
| **Al (%)** | **Si (%)** | **Fe (%)** | **Cu (%)** | **Mn (%)** | **Mg (%)** | **Zn (%)** | **Ni (%)** | **Ti (%)** | **Pb (%)** |
| Bal. | 11.50-13.50 | 0.6 | 0.1 | 0.4 | 0.1 | 0.1 | 0.1 | 0.15 | 0.1 |

All of the experiments were classified into three main phases. These phases, as mentioned before, are thermal analysis, microstructure analysis, and mechanical properties testing. In the first phase, the effect of adding Sn on characteristic parameters of the solidification process, such as the nucleation temperature, growth temperature, and solidus temperature in the α-Al and Al-Si phases was assessed. In the second phase, the effect of adding Sn on microstructure, such as size and shape of the Si particles was investigated, and in the third phase, the effect of adding Sn on mechanical properties, such as hardness was evaluated.

## 3.2 Materials Preparation

To control the parameters of the cooling curve like its rate for thermal analysis in the solidification process, a ceramic crucible was chosen.

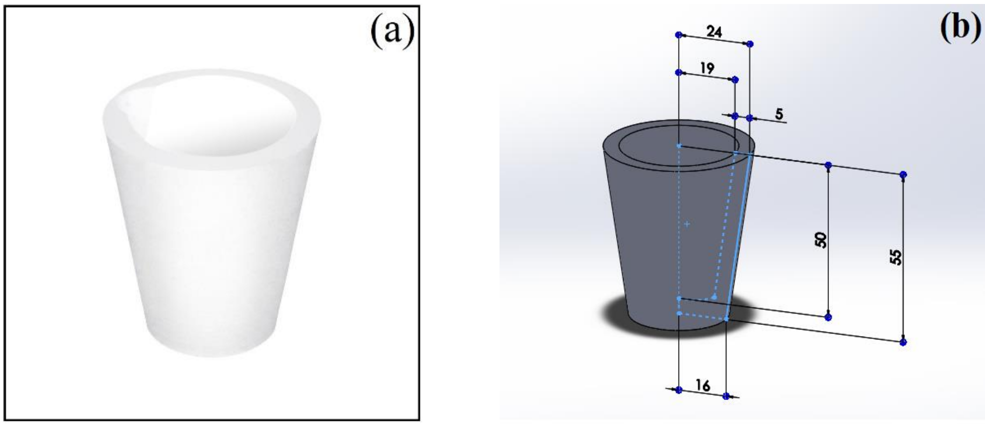

Figure 3.1: (a) The Ceramic Crucible, and (b) Its Dimensions

The ingot was divided into small pieces. Then, they were cleaned and dried to remove any dirt from their surfaces. Later, they were weighted and melted in an electrical furnace. Also, tin as an additive was weighted according to 0.1, 0.5, and 1 wt.%. The additives were wrapped in an aluminum foil, then they were plunged into the molten alloy and stirred to make sure that they dissolved properly all over it.


Figure 3.2: The Ingot of ETIAL-140

The melting temperature was increased to 750-760 °C to provide enough time for the molten alloys (the base alloy and relevant additives) to complete melt homogenization [59]. The melt was stirred, and its surface was skimmed to remove impurities and dross. Alongside the melting process, the ceramic crucible was preheated at 750 °C in a heating furnace to show more transformations during the solidification process.


Figure 3.3: (a) The Electrical Furnace, and (b) The Heating Furnace

## 3.3 Thermal Analysis

Thermal analysis was obtained by using a data acquisition module and an appropriate calibrated K-type thermocouple. The data acquisition module used in this research was OMEGA TC-08. It was a high-speed module with eight thermocouple channels that had a conversion time of 100 ms and a temperature accuracy of ±0.5 ºC. The K-type thermocouple used in this research was PK-1000. It was a thermocouple with high-temperature mineral fiber insulation and a temperature range of -50 to 1000 ºC. This thermocouple was located in the center of the ceramic crucible, 25 mm above its bottom to record the temperature of the center during the solidification process.

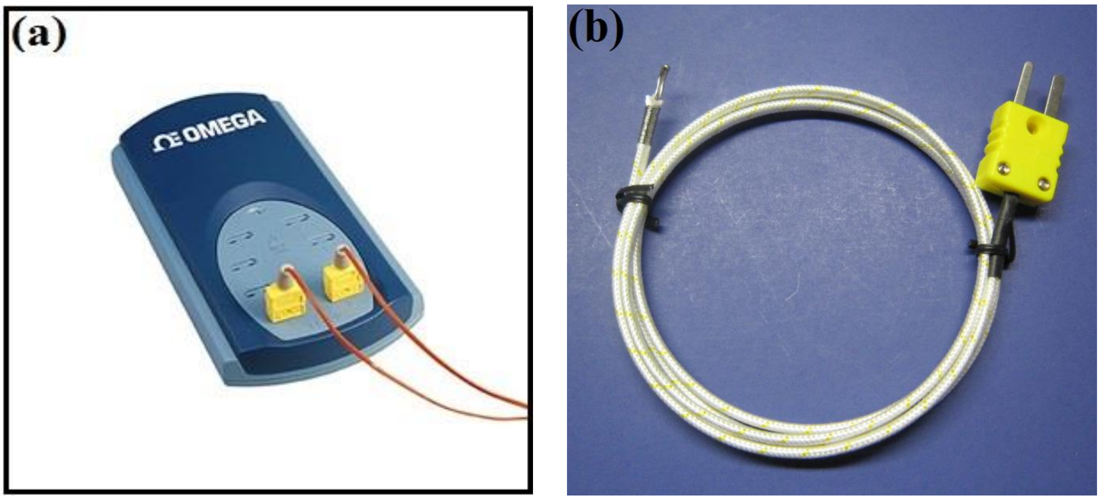

Figure 3.4: (a) The Data Acquisition Module OMEGA TC-08, and (b) The K-type Thermocouple PK-1000

The temperature-time data was recorded and exported to a computer to which the data acquisition module was connected. This data was collected by software that showed any instant observation of cooling curves and monitored any process during the solidification. The software used in this part was PicoLog 6. Later, this data was utilized by data analysis software for further analyses. The software used in this research was FlexPro 9. It was suitable for plotting and smoothing the cooling curves along with the first and second derivative curves (dT/dt and $d^2T/dt^2$). As mentioned before, these derivative curves improved the accuracy of identifying the characteristic parameters of the alloys that could not be recognized on the cooling curves.

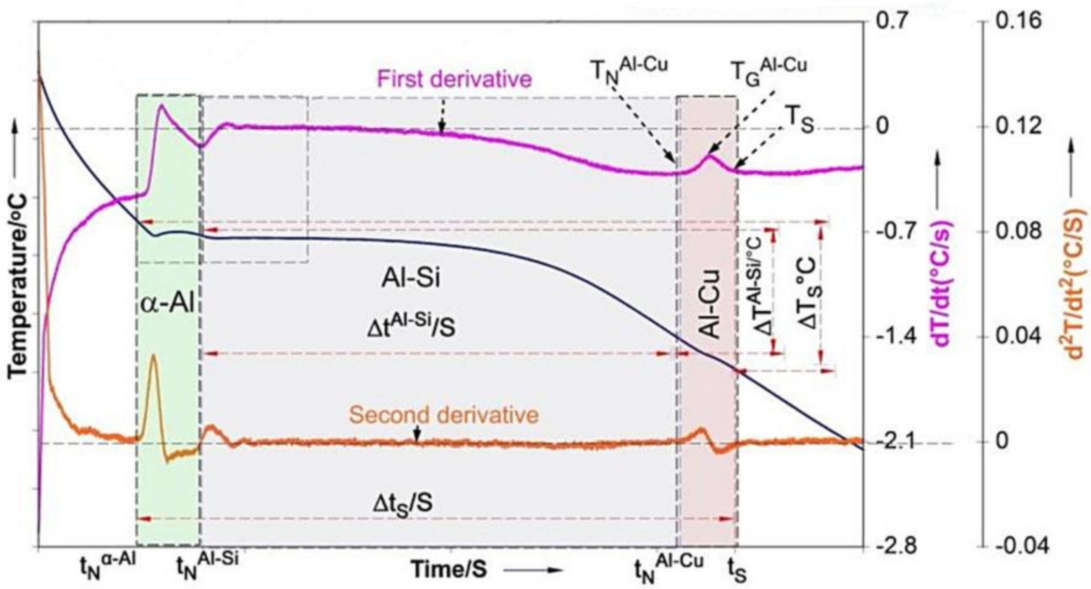

Figure 3.5: Cooling Curve of Al-11Si-Cu-Mg Alloy with its corresponding Derivative Curves plotted and smoothed by using FlexPro 9 [45]

The formation of the α-Al phase starts when the second derivative rises sharply after its intersection with the zero line. It is called nucleation temperature. The $T_N^{\alpha\text{-}Al}$ is the temperature of the first silicon crystals when they nucleate and start to grow (Figure 3.5). In the Al-Si phase, the second derivative decreases, then increases until intersects with the zero line. It is called growth temperature. In this phase, the melt temperature rises to a steady-state $T_G^{Al\text{-}Si}$ (Figure 3.5). Finally, the second derivative decreases, then increases until intersects with the zero line and stabilizes. It is the end of the solidification process with its corresponding temperature, solidus temperature ($T_S$) (Figure 3.5). The characteristic parameters of the solidification process determined by the CA-CCTA technique in this research are shown in Table 3.2.

Table 3.2: Characteristic Parameters of the Solidification examined in this Research

| Symbol | Description |
|---|---|
| $T_N^{\alpha\text{-}Al}$ | Nucleation Temperature of the α-Al Phase |
| $t_N^{\alpha\text{-}Al}$ | Nucleation Time of the α-Al Phase |
| $T_G^{Al\text{-}Si}$ | Growth Temperature of the Al-Si Phase |
| $t_G^{Al\text{-}Si}$ | Growth Time of the Al-Si Phase |
| $T_S$ | Solidus Temperature |
| $t_S$ | Solidus Time |

## 3.4 Microstructural Analysis

For microstructural analysis, samples from the experiments of thermal analysis were prepared and evaluated by using different techniques like Optical Microscopy (OM) and Scanning Electron Microscopy equipped with Energy Dispersive X-ray Spectroscopy (SEM/EDS).

First of all, the specimens were sectioned horizontally from 25 mm above its bottom exactly at the end of the inserted thermocouple. Then, they were mounted in resin. The resin mounted samples were grounded by Silicon Carbide (SiC) papers with various sizes from 200 grit to 1000 grit. Later, the samples were polished by Struers Silica Oxide OP-S. Finally, a normal etching was applied with 5% HF to show the eutectic Si structure.

Characteristic parameters of eutectic Si particles like size and shape were examined by an optical microscope and an image analyzer on the samples of the base alloy and alloys modified with different Sn addition. The optical microscope and image analyzer used in this research were OLYMPUS GX53 (Figure 3.6) and ImageJ. Different zones of optical micrographs were chosen to average 15 measurements and obtain the mean area of the Si particles under 200 µm magnification for each sample.


Figure 3.6: The Optical Microscope OLYMPUS GX53

Elemental maps and identification of elements in the spectrum were studied by a scanning electron microscope on the sample of the alloy modified with 1% Sn addition. The scanning electron microscope used in this research was TESCAN MIRA2-LMU (Figure 3.7). The identification of elements in the spectrum after adding 1% Sn is tabulated with different data like their concentration, their percentage by weight, their atomic percent, etc.

Figure 3.7: The Scanning Electron Microscope TESCAN MIRA2-LMU

## 3.5 Mechanical Properties Analysis

From mechanical properties, hardness was selected to determine the average hardness values (HV) for each sample of the base alloy and alloys modified with different Sn addition. From hardness tests, the Vickers hardness test was selected, and the hardness tester used in this research was Struers Duramin-100 (Figure 3.8) with ISO 6507-1 and ASTM E384 standard test methods. 2.5 kgf was applied with this hardness tester as an applied load, and five tests were done totally. The reported results are the average values of these tests per sample.

Figure 3.8: The Hardness Tester Struers Duramin-100

# Chapter 4

# RESULTS AND DISCUSSION

## 4.1 Introduction

The results of the experiments taken before will be analyzed, in this chapter. These are the thermal analysis results that were recorded by the data acquisition module after tin addition with different percentages. The effect of adding Sn with the microstructural examination of polished samples and the changes of characteristic parameters were assessed. Also, elemental maps and identification of elements in the spectrum after adding 1% Sn was investigated by SEM/EDS.

## 4.2 Thermal Analysis

The cooling curves of the samples are plotted. These samples, as mentioned before, were prepared from base alloy without any additive and with different addition of Sn (0.1, 0.5, and 1%). These curves are shown in Figure 4.1. In this figure, the cooling curves of the samples are compared to each other. As can be seen, tin addition has an effect on the eutectic reaction region of these cooling curves.

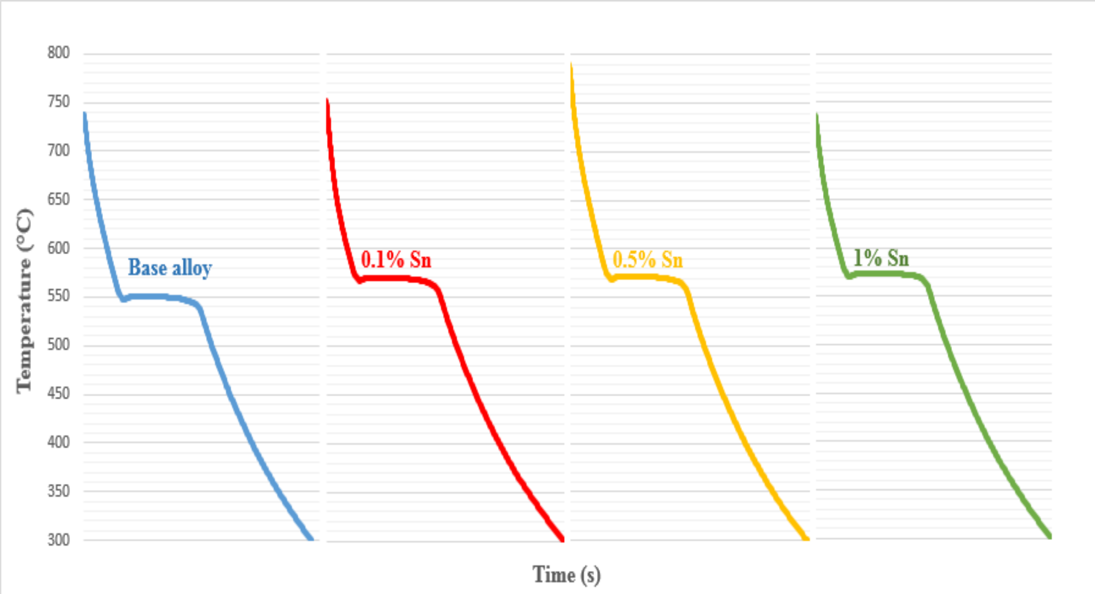

Figure 4.1: Cooling Curves of the Base Alloy and Alloys modified with Different Sn Addition

Also, the characteristic parameters of these cooling curves like the nucleation temperature of the α-Al phase ($T_N^{\alpha\text{-}Al}$), the growth temperature of the Al-Si phase ($T_G^{Al\text{-}Si}$), and the solidus temperature ($T_S$) with their corresponding times are tabulated in Table 4.1 and plotted in Figure 4.2. These parameters were determined by using the first and second derivatives curves, as shown in Figure 4.3, 4.4, 4.5, and 4.6.

Table 4.1: Cooling Curve Characteristic Parameters of the Base Alloy and Alloys modified with Different Sn Addition

| Samples (%) | Characteristic Parameters | | | | | |
|---|---|---|---|---|---|---|
| | Nucleation | | Growth | | Solidus | |
| | $T_N^{\alpha\text{-}Al}$ (°C) | t (s) | $T_G^{Al\text{-}Si}$ (°C) | t (s) | $T_S$ (°C) | t (s) |
| **0%** | 571.05 | 205.7 | 550.67 | 300.5 | 525.41 | 511.5 |
| **0.1%** | 582.68 | 190.7 | 570.09 | 277.3 | 545.25 | 496.1 |
| **0.5%** | 589.28 | 145.9 | 571.88 | 218.3 | 547.42 | 438.2 |
| **1%** | 592.64 | 139.9 | 573.13 | 232.3 | 548.45 | 450.7 |

As can be seen, when Sn increased, the nucleation temperature of the α-Al phase increased. By increasing Sn from 0% to 0.1%, $T_N{}^{\alpha\text{-Al}}$ increased suddenly from 571.05 °C to 582.68 °C. $T_N{}^{\alpha\text{-Al}}$ increased by 6.6, and 3.36 °C upon the addition of 0.5%, and 1% Sn respectively. Also, when Sn increased, the growth temperature of the Al-Si phase increased. By increasing Sn from 0% to 0.1%, $T_G{}^{\text{Al-Si}}$ increased dramatically from 550.67 ºC to 570.09 ºC. $T_G{}^{\text{Al-Si}}$ increased by 1.79, and 1.25 °C upon the addition of 0.5%, and 1% Sn respectively. Similarly, when Sn increased, the temperature at the end of the solidification (the solidus temperature) increased. Like $T_G{}^{\text{Al-Si}}$, by increasing Sn from 0% to 0.1%, $T_S$ increased dramatically from 525.41 ºC to 545.25 ºC. $T_S$ increased by 2.17, and 1.03 °C upon the addition of 0.5%, and 1% Sn respectively. It shows that the addition of elements like tin does not only have an impact on the nucleation and growth temperatures but also on the solidus temperature. It can be observed by increasing Sn, the nucleation of the α-Al phase started earlier in comparison with the base alloy without any additive, and the fastest start was obtained by adding 1% Sn.

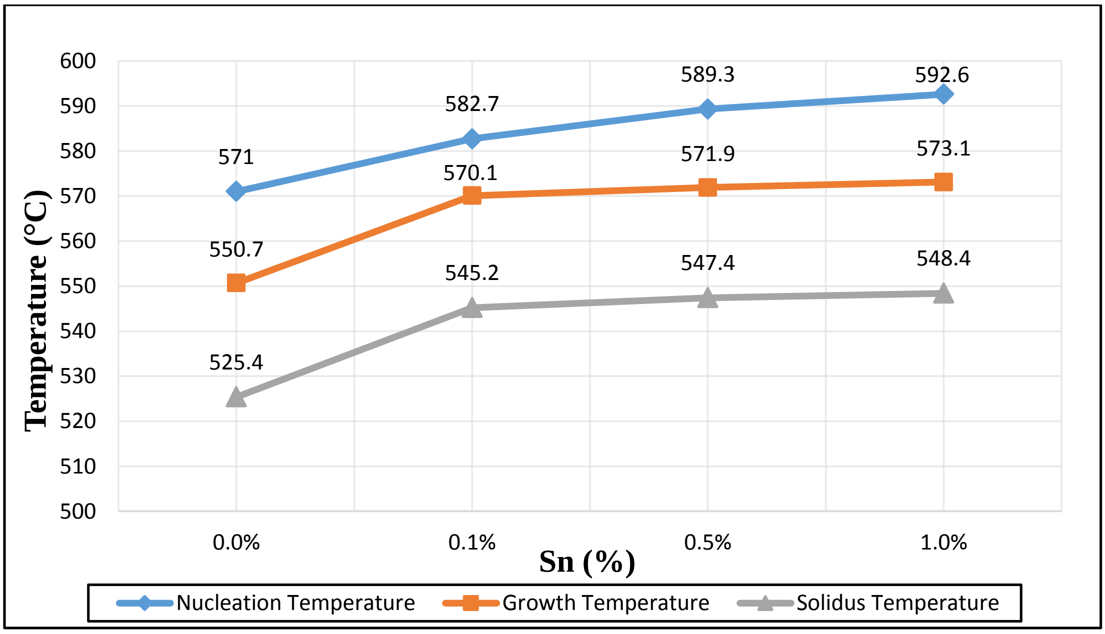


Figure 4.2: Changes in the Nucleation Temperature, Growth Temperature, and Solidus Temperature of the Base Alloy and Alloys modified with Different Sn Addition

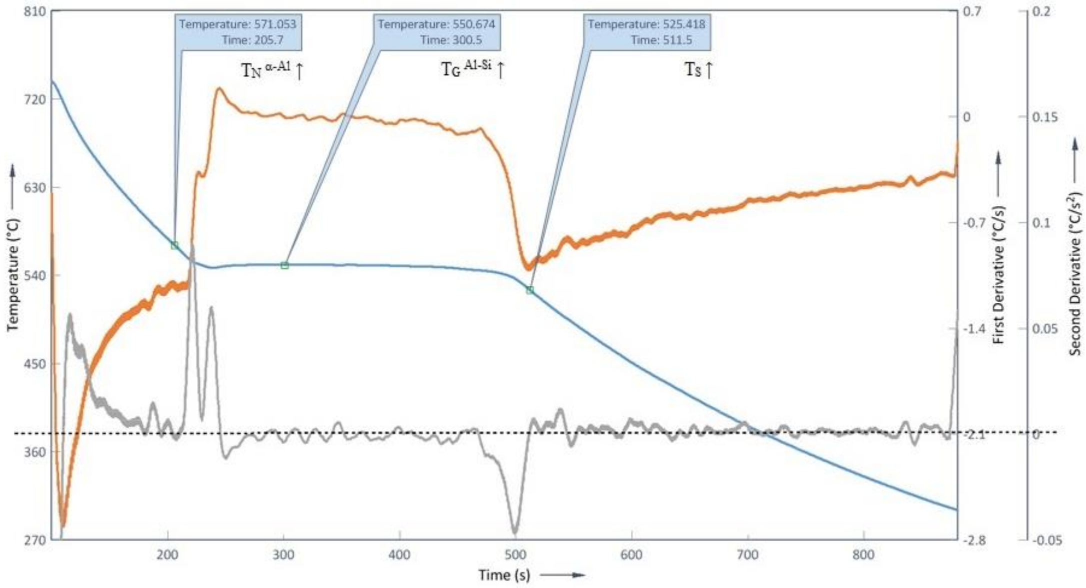


Figure 4.3: Cooling Curve of the Base Alloy with its corresponding Derivative Curves plotted and smoothed by using FlexPro 9

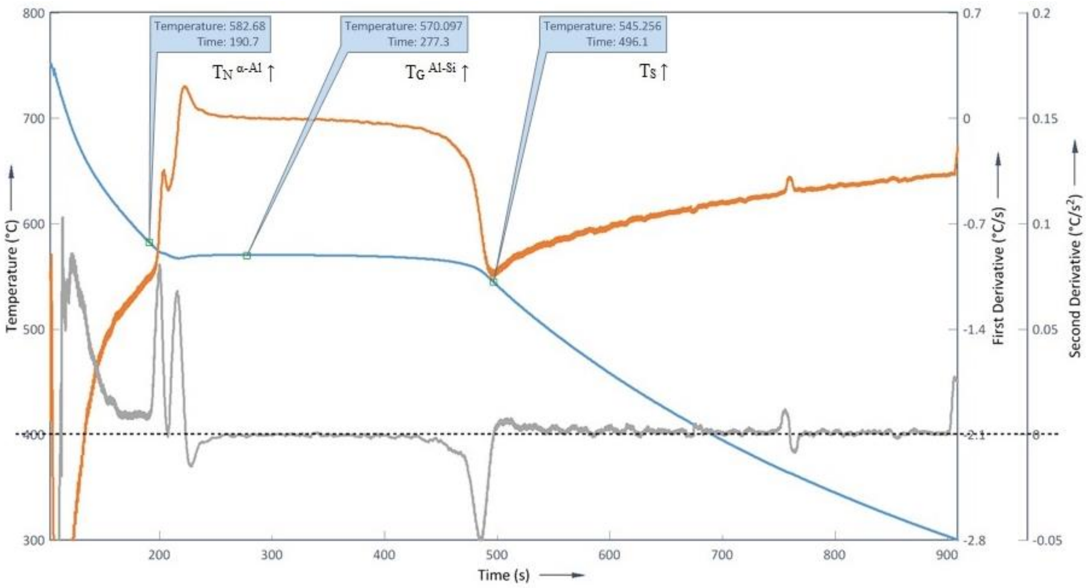


Figure 4.4: Cooling Curve of the Alloy modified with 0.1% Sn with its corresponding Derivative Curves plotted and smoothed by using FlexPro 9

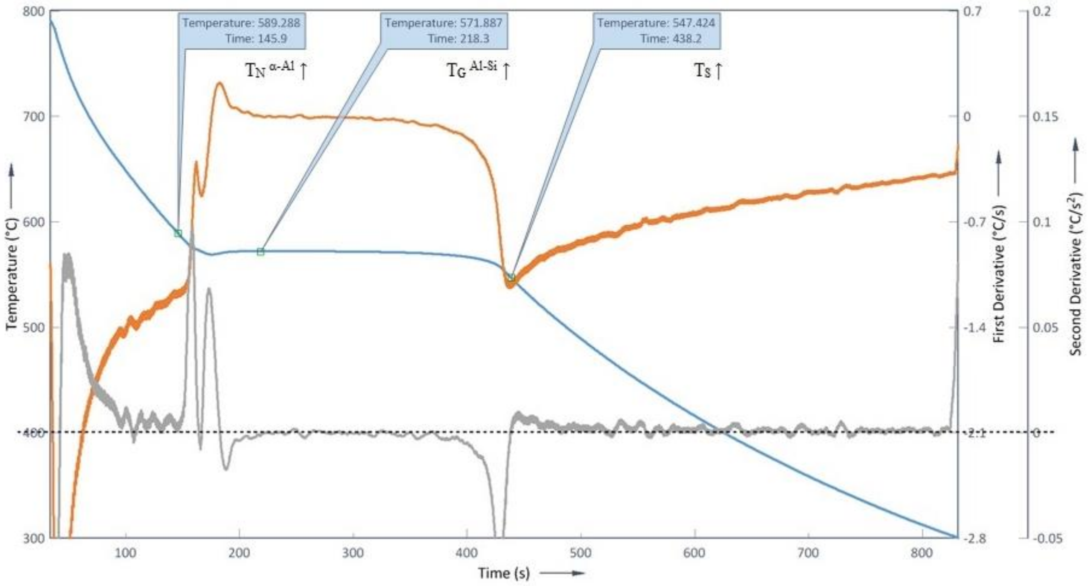


Figure 4.5: Cooling Curve of the Alloy modified with 0.5% Sn with its corresponding Derivative Curves plotted and smoothed by using FlexPro 9

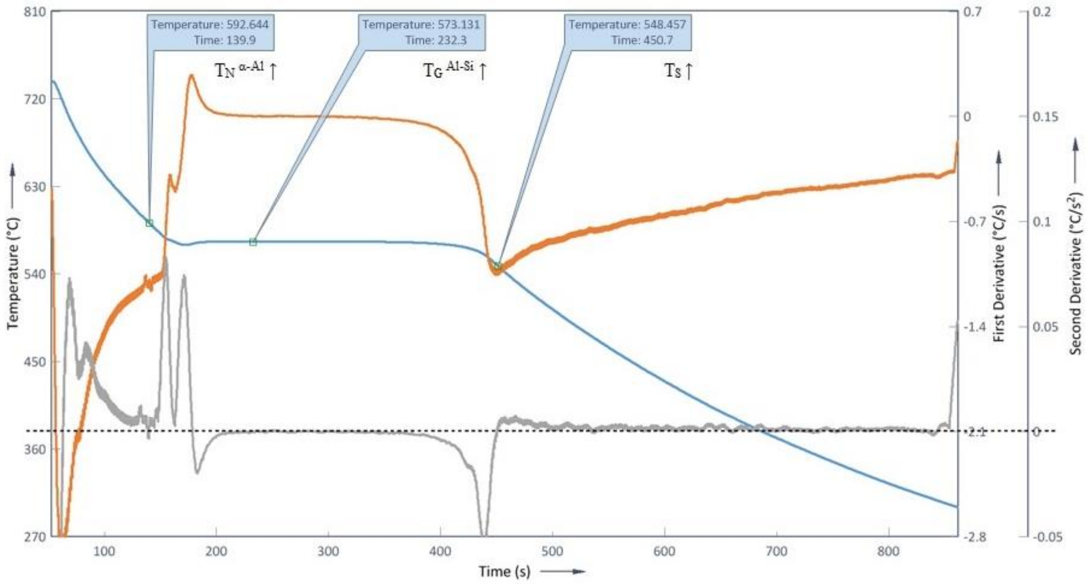


Figure 4.6: Cooling Curve of the Alloy modified with 1% Sn with its corresponding Derivative Curves plotted and smoothed by using FlexPro 9

Based on the characteristic parameters determined before, the total solidification ranges of temperature with its corresponding time can be obtained by these calculations: ($\Delta T = T_N^{\alpha\text{-}Al} - T_S$ and $\Delta t = t_N^{\alpha\text{-}Al} - t_S$). ΔT and Δt is the difference between the start of the α-Al phase nucleation and the end of the solidification process. The results are tabulated in Table 4.2 and plotted in Figure 4.7.

Table 4.2: Total Solidification Ranges of Temperature and Time for the Base Alloy and Alloys modified with Different Sn Addition

| **Samples (%)** | **$\Delta T = T_N^{\alpha\text{-}Al} - T_S$ (°C)** | **$\Delta t = t_N^{\alpha\text{-}Al} - t_S$ (s)** |
|---|---|---|
| **0%** | 45.64 | 305.8 |
| **0.1%** | 37.43 | 292.3 |
| **0.5%** | 41.86 | 305.4 |
| **1%** | 44.19 | 310.8 |

As can be seen, the total solidification temperature (ΔT) and time (Δt) decreased with 0.1% addition of Sn, then increased by adding Sn up to 1%. The decrease of ΔT and Δt upon the addition of Sn could be due to the effect of Sn solubility on the first phase, α-Al [60]. In modified alloys, the solid phase formed slower at the early stages compared to unmodified alloy (the base alloy without any additive). Because of the low solubility of Sn in aluminum, the added Sn during the solidification concentrated at the first phase, α-Al [60]. It caused to form a new Al-Sn phase that dissolving it is difficult at high temperatures. Based on the obtained results, the most decrease of ΔT and Δt occurred by adding 0.1% Sn.

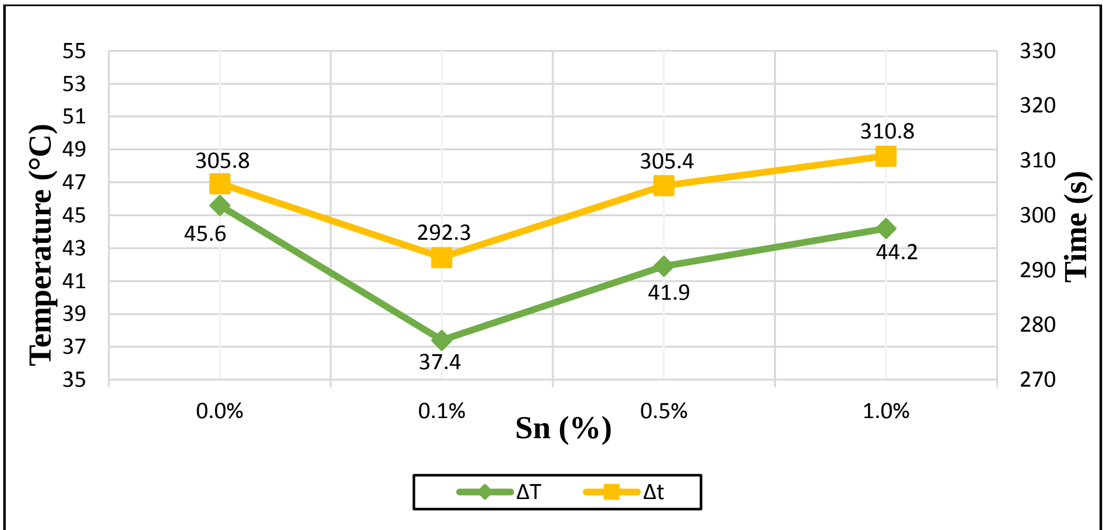


Figure 4.7: Changes in the Total Solidification Ranges of Temperature and Time for the Base Alloy and Alloys modified with Different Sn Addition

## 4.3 Microstructural Analysis

The optical micrographs of the base alloy and with different level of Sn concentrations are shown in Figure 4.8. This figure demonstrates differences in the microstructure like the size and shape of particles of the eutectic Si structure.

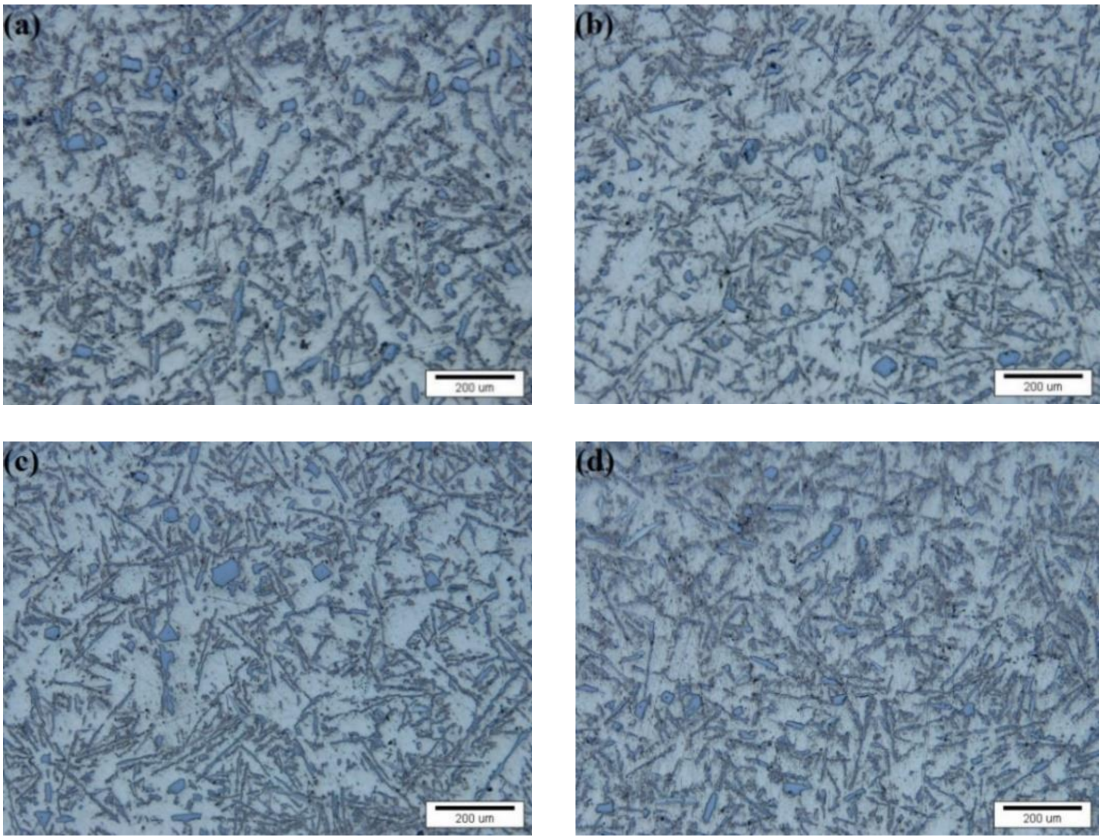


Figure 4.8: Optical Micrographs of (a) The Base Alloy, (b) 0.1 wt.% Sn, (c) 0.5 wt.% Sn, and (d) 1 wt.% Sn

As can be seen, the Si particles of the base alloy had a plate-like, flaky, and needle-shaped (acicular) form. By the addition of 0.1% Sn, the number of Si plates and needle-shaped particles slightly decreased but no noticeable changes in their size were observed. By increasing Sn to 0.5%, the Si plates size slightly increased and also the number of needle-shaped particles increased. After Adding 1% Sn, the Si plates size slightly decreased but the number of them increased. No noticeable changes in the number of needle-shaped particles were observed. It needs to be mentioned those needle-shaped particles had irregular and longitudinal structures. These results show Sn does not have any effect on the modification of the Al-Si alloy.

The mean area of particles of the eutectic Si structure was measured. The results are tabulated in Table 4.3 and plotted in Figure 4.9. Although the size of the Si particles fluctuated by increasing Sn, their mean area increased.

Table 4.3: Mean Area of Si Particles with their corresponding Standard Deviation for the Base Alloy and Alloys modified with Different Sn Addition

| **Samples (%)** | **Mean Area (μm$^2$)** | **SD** |
|---|---|---|
| **0%** | 120.034 | 5.715 |
| **0.1%** | 118.163 | 6.226 |
| **0.5%** | 119.653 | 5.343 |
| **1%** | 124.147 | 3.181 |

As can be seen, the mean area of Si particles in the base alloy was 120.034 μm$^2$. By adding 0.1% Sn, the mean area decreased to 118.163 μm$^2$. Then by increasing Sn up to 1%, the mean area increased. By increasing Sn, the growth temperature of the Al-Si phase increased. The temperature increment does not lead to Si structure modification. Because when the temperature increased, the mean area of Si particles increased. It means that Sn does not have any effect on the modification of this type of Al-Si alloy.

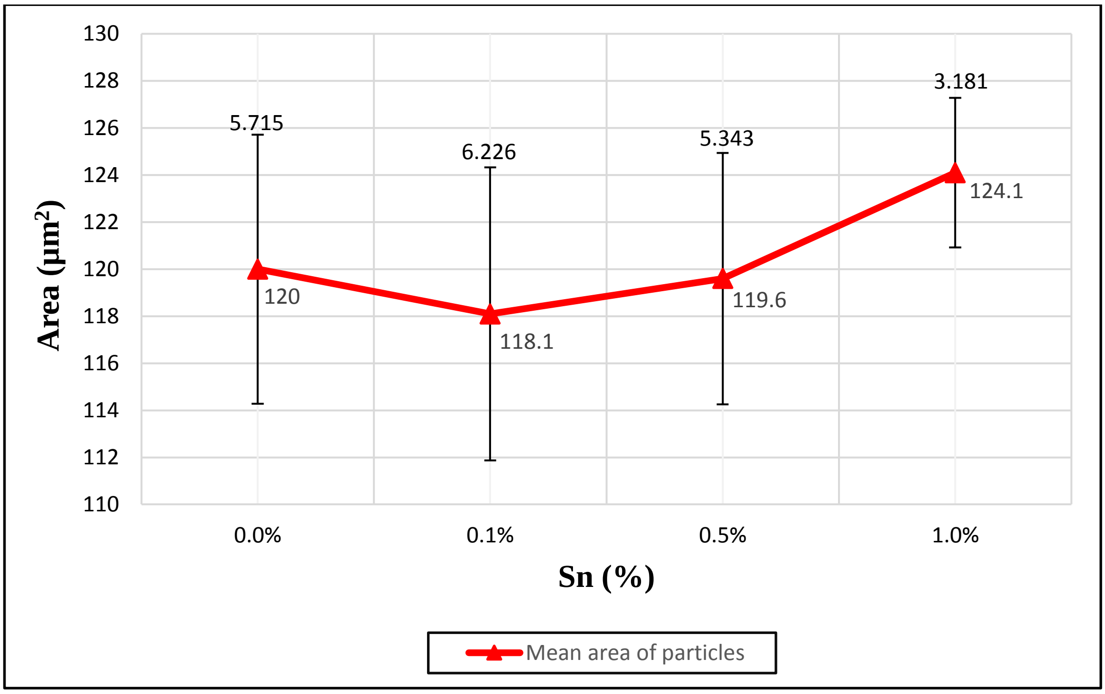


Figure 4.9: Changes in the Mean Area of Si Particles for the Base Alloy and Alloys modified with Different Sn Addition

The EDS mapping images of the sample from alloy modified with 1% Sn are shown in Figure 4.10. These images were used to identify and analyze the chemical composition present in the alloy. Besides, The SEM image and EDS point analysis corresponding to the location marked (Spectrum 4) used to identify the Sn phases present in the sample from alloy modified with 1% Sn are shown in Figure 4.11. Also, the table of contents of the Spectrum 4 is shown in Table 4.4.

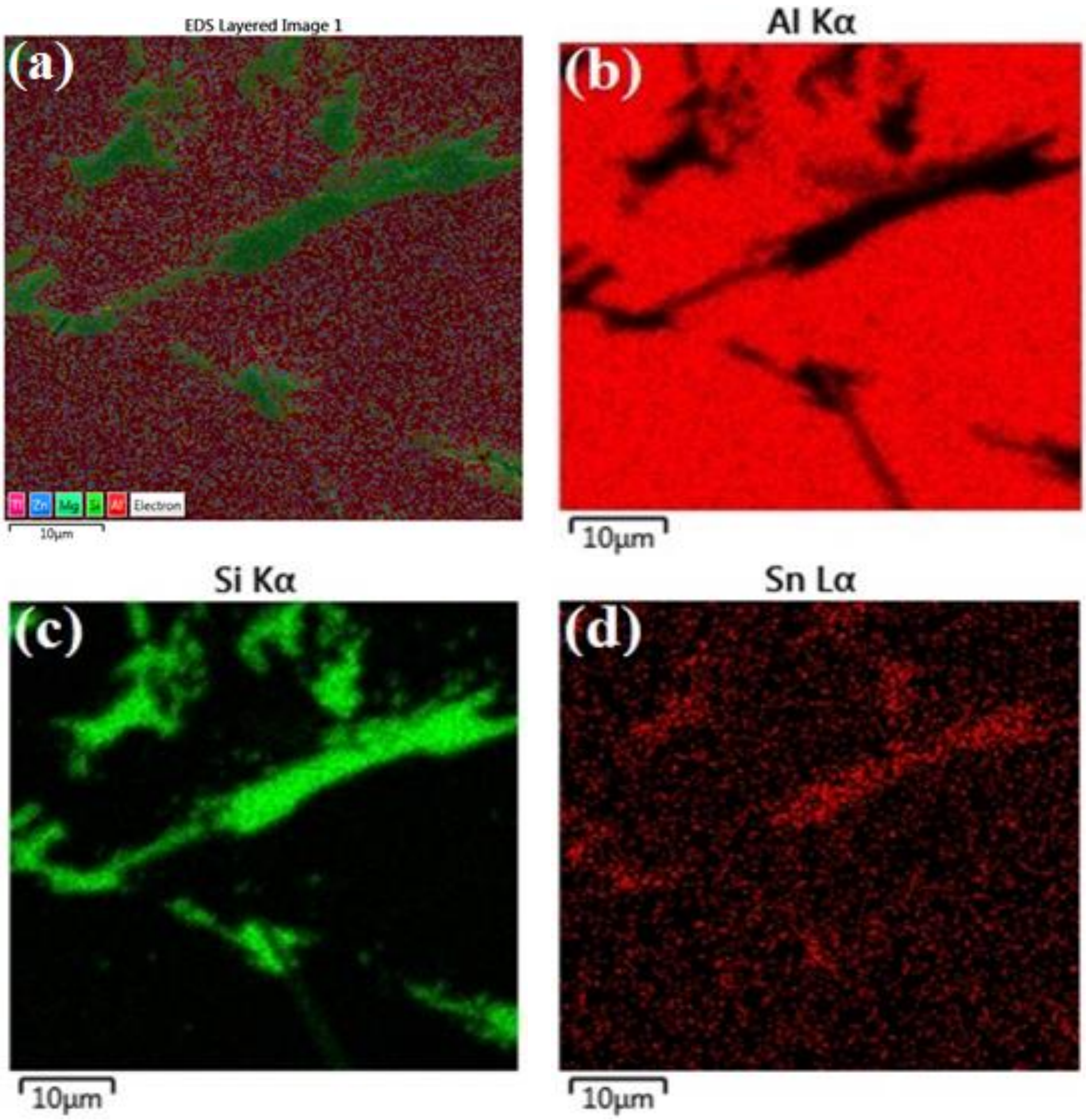


Figure 4.10: EDS Mapping Images of the Sample from Alloy modified with 1% Sn (a) EDS Layered Image, (b) Al Compound, (c) Si Compound, and (d) Sn Compound

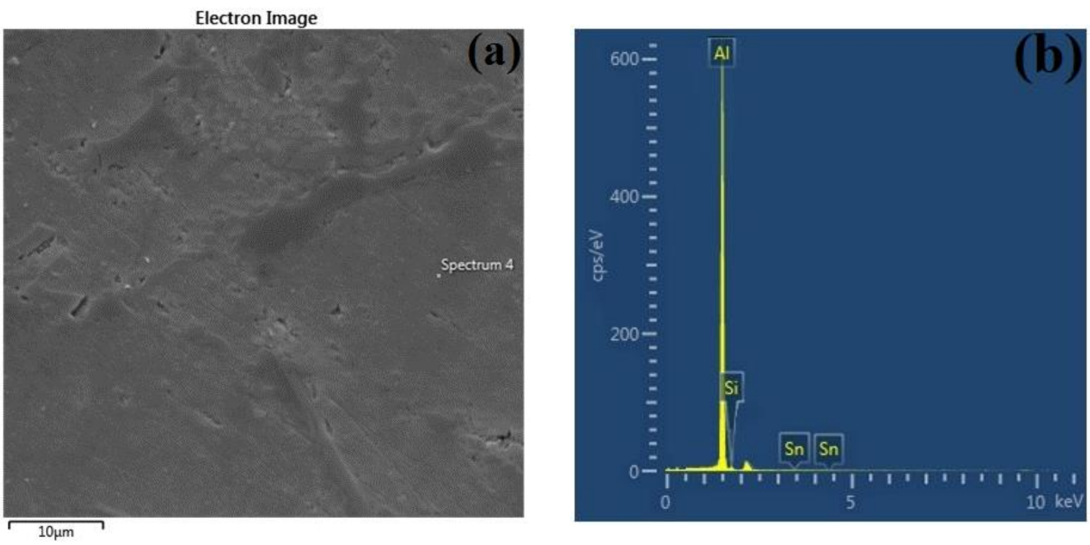


Figure 4.11: (a) SEM Image and Location of the Spectrum 4, and (b) EDS Point Analysis of the Sample from Alloy modified with 1% Sn (Spectrum 4)

As mentioned before, by increasing Sn, the solidus temperature of the last solidification phase increased. The reaction temperature later was increased by the formation of intermetallic compounds. Because Sn formed the intermetallic compound with Al and Si. From the EDS point analysis and its corresponding table of contents can be observed this intermetallic compound is like a ternary compound (Al-Si-Sn). As can be seen, these intermetallic compounds have a plate-like structure.

Table 4.4: Table of Contents of the Spectrum 4

| Element | Line Type | Apparent Concentration | wt.% | Atomic % | Standard Label |
|---|---|---|---|---|---|
| Al | K series | 44.81 | 89.89 | 81.31 | $Al_2O_3$ |
| Si | K series | 0.29 | 1.15 | 1.00 | $SiO_2$ |
| Cu | L series | 0.01 | 0.04 | 0.01 | Cu |
| Zn | L series | 0.02 | 0.05 | 0.02 | Zn |
| Sn | L series | 0.54 | 8.87 | 17.66 | Sn |
| Total: | | | 100.0 | 100.0 | |

## 4.4 Mechanical Properties Analysis

The mechanical properties of Al-Si alloys are controlled by several parameters such as characteristics of eutectic Si particles, the addition of alloying elements, etc. [57]. Hardening phases form during the solidification process and their size, type, and also distribution depends on the addition of alloying elements and chemical composition of the alloy. Also, determining the values of strength and hardness depends on the intermetallic phases and Si particles present in the microstructure [58]. Modifying the morphology of Si particles of unmodified alloys may result in an increment of the hardness values.

Here, the effect of Sn addition on the mechanical properties was studied by doing a hardness test. The results are tabulated in Table 4.5 and plotted in Figure 4.12. This table shows the hardness values for the base alloy and alloys modified with different Sn addition.

Table 4.5: Results of the Hardness Test for the Base Alloy and Alloys modified with Different Sn Addition

| **Samples (%)** | **#1 (HV)** | **#2 (HV)** | **#3 (HV)** | **#4 (HV)** | **#5 (HV)** | **Average (HV)** |
|---|---|---|---|---|---|---|
| **0%** | 53.9 | 53.4 | 54.0 | 53.6 | 53.7 | 53.72 |
| **0.1%** | 54.9 | 55.1 | 54.7 | 54.7 | 55.2 | 54.92 |
| **0.5%** | 56.8 | 57.6 | 57.4 | 57.9 | 57.3 | 57.40 |
| **1%** | 58.8 | 58.3 | 59.1 | 59.3 | 58.9 | 58.88 |

As can be seen, when Sn increased, the average value of hardness slightly increased. The hardness value of the base alloy without any additive was measured 53.72 HV. Then, by increasing Sn up to 1%, the hardness value slightly increased. As mentioned before, Sn formed the intermetallic compound with Al and Si. Therefore, hardness increasing with Sn increasing was because of the solid and hard intermetallic compound formed between Sn, Al, and Si in the last phase of the solidification process.

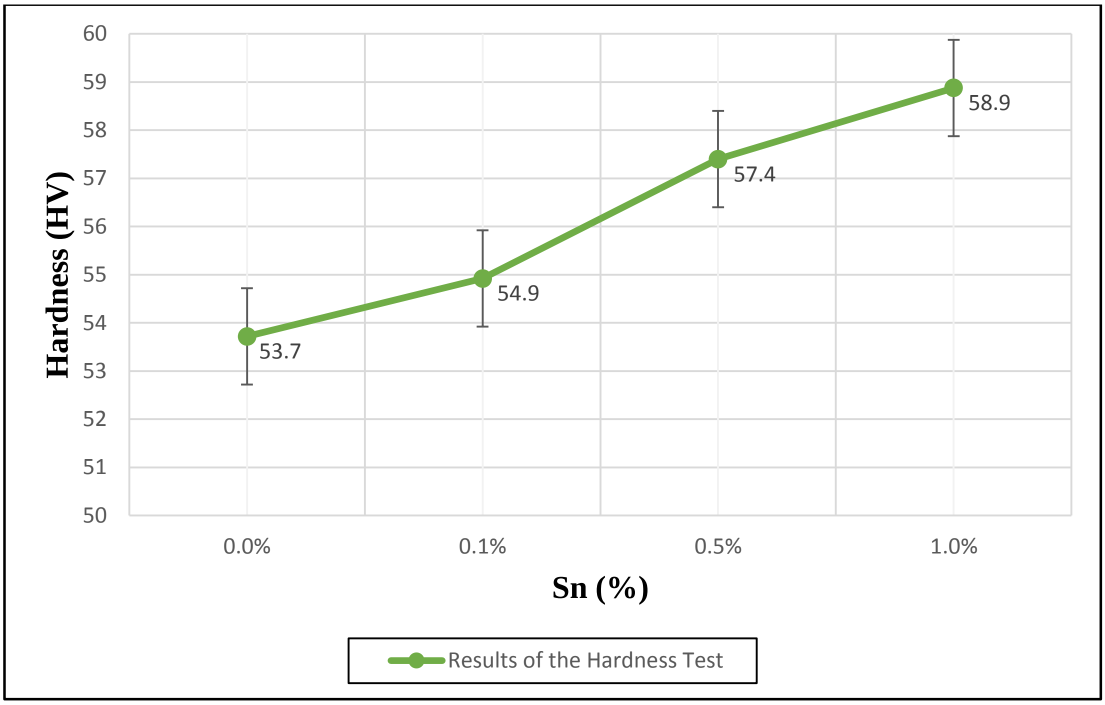


Figure 4.12: Changes in the Results of the Hardness Test for the Base Alloy and Alloys modified with Different Sn Addition

# Chapter 5

# CONCLUSION

## 5.1 Introduction

In the previous chapter, the results of the experiments were analyzed and discussed. In this chapter, the summary of them will be covered.

## 5.2 Conclusion

According to the results, these conclusions were obtained:

1) By increasing Sn, the nucleation of the α-Al phase started earlier in comparison with the base alloy without any additive, and the fastest start was obtained by adding 1% Sn.

2) The decrease of ΔT and Δt upon the addition of Sn could be due to the effect of Sn solubility on the first phase, α-Al. In modified alloys, the solid phase formed slower at the early stages compared to unmodified alloy (the base alloy without any additive). Because of the low solubility of Sn in aluminum, the added Sn during the solidification concentrated at the first phase, α-Al. It caused to form a new Al-Sn phase that dissolving it is difficult at high temperatures. Based on the obtained results, the most decrease of ΔT and Δt occurred by adding 0.1% Sn.

3) The Si particles of the base alloy had a plate-like, flaky, and needle-shaped (acicular) form. By the addition of 0.1% Sn, the number of Si plates and needle-shaped particles slightly decreased but no noticeable changes in their size were observed. By

increasing Sn to 0.5%, the Si plates size slightly increased and also the number of needle-shaped particles increased. After Adding 1% Sn, the Si plates size slightly decreased but the number of them increased. No noticeable changes in the number of needle-shaped particles were observed. It needs to be mentioned those needle-shaped particles had irregular and longitudinal structures. These results show Sn does not have any effect on the modification of the Al-Si alloy.

4) By increasing Sn, the temperature of the Al-Si phase increased. The temperature increment does not lead to Si structure modification. Because when the temperature increased, the mean area of Si particles increased. It means that Sn does not have any effect on the modification of this type of Al-Si alloy.

5) By increasing Sn, the temperature of the last solidification phase increased. The reaction temperature later was increased by the formation of intermetallic compounds. Because Sn formed the intermetallic compound with Al and Si. From the EDS point analysis and its corresponding table of contents can be observed this intermetallic compound is like a ternary compound (Al-Si-Sn). As can be seen, these intermetallic compounds have a plate-like structure.

6) Hardness increasing with Sn increasing was because of the solid and hard intermetallic compound formed between Sn, Al, and Si in the last phase of the solidification process.

# REFERENCES


[1] Ball, W. D., Hill, W. J., & Scott, J. R. (2011). Introduction to Chemistry: General, Organic and Biological.

[2] Sritharan, T., & Li, H. (1997). Influence of titanium to boron ratio on the ability to grain refine aluminum-silicon alloys. *Journal of Materials Processing Technology*, *63*(1-3), 585-589.

[3] Kaufman, J. G. (2000). *Introduction to aluminum alloys and tempers*. ASM International.

[4] Kaufman, J. G., & Rooy, E. L. (2004). *Aluminum alloy castings: properties, processes, and applications*. ASM International.

[5] Hernandez, F. C. R., Ramírez, J. M. H., & Mackay, R. (2017). *Al-Si alloys: automotive, aeronautical, and aerospace applications*. Springer.

[6] Totten, G. E., & MacKenzie, D. S. (Eds.). (2003). *Handbook of Aluminum: Volume 2: Alloy Production and Materials Manufacturing* (Vol. 2). CRC press.

[7] Hatch, J. E. (1984). Aluminum: properties and physical metallurgy, vol. 5. *Materials Park (OH): American Society for Metals*, 153.

[8] https://www.azom.com/article.aspx?ArticleID=2863

[9] https://www.azom.com/article.aspx?ArticleID=1446

[10] Gruzleski, J. E., & Closset, B. M. (1990). *The treatment of liquid aluminum-silicon alloys*. American Foundrymen's Society.

[11] Campbell, J. (2003). *Castings*. Elsevier.

[12] Bäckerud, L., Chai, G., & Tamminen, J. (1990). *Solidification characteristics of aluminum alloys: Foundry Alloys*. American Foundrymen's Society.

[13] Bäckerud, L., Chai, G., & Tamminen, J. (1990). *Solidification characteristics of aluminum alloys: Wrought Alloys*. American Foundrymen's Society.

[14] ASM International. Handbook Committee (Ed.). (1990). *Properties and selection: nonferrous alloys and special-purpose materials* (Vol. 2). ASM International

[15] Jorstad, J. L. (1971). The hypereutectic aluminum-silicon alloy used to cast the Vega engine block. *Modern Casting*, *60*(4), 59-64.

[16] Hernandez, R., & Carlos, F. (2004). *Improvement in functional characteristics of aluminum-silicon cast components through the utilization of a novel electromagnetic treatment of liquid melts* (Vol. 68, No. 12).

[17] Wayne, M. (1964). *U.S. Patent No. 3,128,176*. Washington, DC: U.S. Patent and Trademark Office.

[18] Altenpohl, D. G. (1998). Aluminum: Technology, Applications, and Environment, The Minerals. *Metals and Materials Society, Warrendale, PA*, 135.

[19] Mondolfo, L. F. (2013). *Aluminum alloys: structure and properties*. Elsevier.

[20] Hegde, S., & Prabhu, K. N. (2008). Modification of eutectic silicon in Al-Si alloys. *Journal of materials science*, *43*(9), 3009-3027.

[21] Dahle, A. K., Nogita, K., McDonald, S. D., Dinnis, C., & Lu, L. (2005). Eutectic modification and microstructure development in Al-Si Alloys. *Materials Science and Engineering: A*, *413*, 243-248.

[22] Ebhota, W. S., & Jen, T. C. (2017). Effects of Modification Techniques on Mechanical Properties of Al-Si Cast Alloys. In *Aluminum Alloys-Recent Trends in Processing, Characterization, Mechanical Behavior and Applications*. IntechOpen.

[23] Warren A. (1997). Phase Diagrams: Solidification of Al-Si Alloys. The University of Southampton.

[24] Jorstad, J. L., Rasmussen, W. M., & Zalensas, D. L. (1993). Aluminum Casting Technology, American Foundrymen's Society. *Inc., Des Plaines, IL, USA*.

[25] Chang, J. Y., & Ko, H. S. (2000). Twin probability of eutectic Si in rare-earth modified Al-7wt% Si alloy. *Journal of Materials Science Letters*, *19*(3), 197-199.

[26] Lu, S. Z., & Hellawell, A. (1987). The mechanism of silicon modification in aluminum-silicon alloys: impurity induced twinning. *Metallurgical Transactions A*, *18*(10), 1721-1733.

[27] Bourcier, G. F., Dickinson, J., Tessandori, J., & Schiffer, D. (1985). Aluminum recycling casebook. *The Aluminum Association Inc*, 56.

[28] MacKay, R., & Sokolowski, J. (2010). Comparison between wedge test castings and component engine block casting properties. *International Journal of Metalcasting*, *4*(4), 33-50.

[29] Mackay, R., & Sokolowski, J. (2008). Experimental observations of dendrite coarsening & Al-Si eutectic growth in progressively quenched structures of Al-Si-Cu casting alloys. *International Journal of Metalcasting*, *2*(2), 57-75.

[30] Djurdjevic, M., Stockwell, T., & Sokolowski, J. (1999). The effect of strontium on the microstructure of the aluminum silicon and aluminum copper eutectics in the 319 aluminum alloy. *International Journal of Cast Metals Research*, *12*(2), 67-73.

[31] Paray, F., & Gruzleski, J. E. (1994). Factors to Consider in Modification (94-115). *Transactions of the American Foundrymen's Society*, *102*, 833-842.

[32] Zamani, M., & Seifeddine, S. (2016). Determination of Optimum Sr Level for Eutectic Si Modification in Al–Si Cast Alloys Using Thermal analysis and Tensile Properties. *International Journal of Metalcasting*, *10*(4), 457-465.

[33] Golbahar, B., Samuel, E., Samuel, A. M., Doty, H. W., & Samuel, F. H. (2014). On thermal analysis, macrostructure and microstructure of grain refined Al–Si–Mg cast alloys: role of Sr addition. *International Journal of Cast Metals Research*, *27*(5), 257-266.

[34] Hernandez, F. R., & Sokolowski, J. H. (2006). Thermal analysis and microscopical characterization of Al–Si hypereutectic alloys. *Journal of Alloys and Compounds*, *419*(1-2), 180-190.

[35] Riddle, Y. W., & Makhlouf, M. M. (2003). Characterizing solidification by non-equilibrium thermal analysis. In *Magnesium Technology 2003 as held at the 2003 TMS Annual Meeting* (pp. 101-106).

[36] Emadi, D., Whiting, L. V., Nafisi, S., & Ghomashchi, R. (2005). Applications of thermal analysis in quality control of solidification processes. *Journal of thermal analysis and calorimetry*, *81*(1), 235-242.

[37] Mohammed. Bsher. A. Asmael. (2015). *The Characterisation of Al-Si-Cu-Mg Eutectic Cast Alloy with Addition of Cerium and Lanthanum* (Doctoral dissertation, Universiti Tun Hussein Onn Malaysia).

[38] G. E., & B. (1997). Qualification of solidification characteristics of Al-Si alloys by thermal analysis. *Master Thesis, Windsor*.

[39] Ye, H. (2003). An overview of the development of Al-Si-alloy based material for engine applications. *Journal of Materials Engineering and Performance*, *12*(3), 288-297.

[40] Knuutinen, A., Nogita, K., McDonald, S. D., & Dahle, A. K. (2001). Modification of Al–Si alloys with Ba, Ca, Y and Yb. *Journal of light metals*, *1*(4), 229-240.

[41] Shin, J. S., & Lee, Z. H. (2004). Computer-aided cooling curve analysis of A356 aluminum alloy. *Metals and Materials International*, *10*(1), 89-96.

[42] Farahany, S., Ourdjini, A., Idris, M. H., & Shabestari, S. G. (2013). Computer-aided cooling curve thermal analysis of near eutectic Al–Si–Cu–Fe alloy. *Journal of thermal analysis and calorimetry*, *114*(2), 705-717.

[43] Ibarra, D. G. (1999). *Control of grain refinement of AI-Si alloys by thermal analysis* (Doctoral dissertation, Tese doutoramento).

[44] Mohamed, A. M. A., Samuel, F. H., Samuel, A. M., Doty, H. W., & Valtierra, S. (2008). Influence of Tin addition on the microstructure and mechanical properties of Al-Si-Cu-Mg and Al-Si-Mg casting alloys. *Metallurgical and materials transactions A*, *39*(3), 490-501.

[45] Ahmad, R., & Asmael, M. B. A. (2016). Influence of lanthanum on solidification, microstructure, and mechanical properties of eutectic Al-Si piston alloy. *Journal of Materials Engineering and Performance*, *25*(7), 2799-2813.

[46] Ahmad, R., Asmael, M. B. A., Shahizan, N. R., & Gandouz, S. (2017). Reduction in secondary dendrite arm spacing in cast eutectic Al–Si piston alloys by cerium addition. *International Journal of Minerals, Metallurgy, and Materials*, *24*(1), 91-101.

[47] Mao, F., Yan, G., Xuan, Z., Cao, Z., & Wang, T. (2015). Effect of Eu addition on the microstructures and mechanical properties of A356 aluminum alloys. *Journal of Alloys and Compounds*, *650*, 896-906.

[48] Tang, Q., Zhao, J., Wang, T., Chen, J., & He, K. (2018). The effects of neodymium addition on the intermetallic microstructure and mechanical properties of Al-7Si-0.3 Mg-0.3 Fe alloys. *Journal of Alloys and Compounds*, *741*, 161-173.

[49] Xu, C., Xiao, W., Hanada, S., Yamagata, H., & Ma, C. (2015). The effect of scandium addition on microstructure and mechanical properties of Al–Si–Mg alloy: A multi-refinement modifier. *Materials Characterization*, *110*, 160-169.

[50] Pramod, S. L., Rao, A. P., Murty, B. S., & Bakshi, S. R. (2016). Effect of Sc addition and T6 aging treatment on the microstructure modification and mechanical properties of A356 alloy. *Materials Science and Engineering: A*, *674*, 438-450.

[51] Farahany, S., Ourdjini, A., Bakar, T. A. A., & Idris, M. H. (2014). A new approach to assess the effects of Sr and Bi interaction in ADC12 Al–Si die casting alloy. *Thermochimica Acta*, *575*, 179-187.

[52] Farahany, S., Idris, M. H., & Ourdjini, A. (2014). Evaluations of antimony and strontium interaction in an Al–Si–Cu–Zn die cast alloy. *Thermochimica Acta*, *584*, 72-78.

[53] Ahmad, R., & Asmael, M. B. A. (2016). Influence of cerium on microstructure and solidification of eutectic Al–Si piston alloy. *Materials and Manufacturing Processes*, *31*(15), 1948-1957.

[54] Mao, F., Yan, G., Li, J., Wang, T., & Cao, Z. (2016). The interaction between Eu and P in high purity Al-7Si alloys. *Materials Characterization*, *120*, 129-142.

[55] Hu, Z., Dong, Z., Yin, Z., Yan, H., Tian, J., & Xie, H. (2018). Solidification behavior, microstructure and silicon twinning of Al-10Si alloys with ytterbium addition. *Journal of Rare Earths*, *36*(6), 662-668.

[56] Ibrahim, M. F., Alkahtani, S. A., Abuhasel, K. A., & Samuel, F. H. (2015). Microstructural characterization of beryllium treated Al-Si alloys. *Advances in Materials Science and Engineering*, *2015*.

[57] Dobrzañski, L. A., Maniara, R., & Sokolowski, J. H. (2007). The effect of cooling rate on microstructure and mechanical properties of AC AlSi9Cu alloy. *Archives of Materials Science*, *106*, 106.

[58] Ibrahim, M. F., Samuel, E., Samuel, A. M., Al-Ahmari, A. M. A., & Samuel, F. H. (2011). Metallurgical parameters controlling the microstructure and hardness of Al–Si–Cu–Mg base alloys. *Materials & Design*, *32*(4), 2130-2142.

[59] Farahany, S., Ourdjini, A., Idrsi, M. H., & Shabestari, S. G. (2013). Evaluation of the effect of Bi, Sb, Sr and cooling condition on eutectic phases in an Al–Si–Cu alloy (ADC12) by in situ thermal analysis. *Thermochimica Acta*, *559*, 59-68.

[60] Dorward, R. C. (1976). The solubility of tin in aluminum. *Metallurgical and Materials Transactions A*, *7*(2), 308-310.